Supplementary material

Ambient Synthesis of Single-Atom catalysts on Catalytically Active Cells for Chemoenzymatic Cascades

Yuqing Zhang,[a] Xiaoyang Yue,*[a] Shuling Zhang,[a] Weixi Kong,[a] [b] Ruijia Zhu,[a] Liya Zhou,[a] Jing Gao,[a] Yanjun Jiang*[a] and Yunting Liu*[a]

[a]*School of Chemical Engineering and Technology, Hebei University of Technology, Tianjin 300401, China*

[b]*Department of Electrical Engineering, Hebei Vocational University of Technology and Engineering, Xingtai 054000, China*

*Corresponding authors e-mail addresses:

xiaoyang.yue@hebut.edu.cn; yanjunjiang@hebut.edu.cn; ytliu@hebut.edu.cn

Contents

1. Chemicals and materials

All chemicals were commercial and used without further purification unless otherwise stated. Sodium tetrachloropalladate, benzylacetone and other related reagents were purchased from Aladdin Chemical Co Ltd (Shanghai, China) and McLean Biochemical Technology Co Ltd (Shanghai, China). NADH-dependent medium-chain alcohol dehydrogenase (ADHa) from *Rhodococcus ruber* is used.

2. Characterization

Powder X-ray diffraction (PXRD) patterns were recorded using Bruker AXS D8. Fourier transform infrared spectra (FT-IR) were obtained on Bruker VECTOR22 spectrometer using KBr as reference. X-ray photoelectron spectroscopy (XPS) was performed by Thermo Scientific K-Alpha X-ray photoelectron spectrometer. The microstructure was characterized by transmission electron microscope (TEM, FEI Talos F200S) and (Spectra Ultra) Double Cs-Corrected TEM (JEM-ARM300F). The contents of Pd were quantified by an Agilent 5110 inductively coupled plasma optical emission spectrometry (ICP-OES). NMR spectra were recorded using a Bruker AV 400 spectrometer. Pd K-edge analysis was performed with Si (111) crystal monochromators at the BL14W1 beamlines at the Shanghai Synchrotron Radiation Facility (SSRF) (Shanghai, China). Before the analysis at the beamline, samples were pressed into thin sheets with 1 cm in diameter and sealed using Kapton tape film. The XAFS spectra were recorded at room temperature using a 4-channel Silicon Drift Detector (SDD) Bruker 5040. Pd K-edge extended X-ray absorption fine structure (EXAFS) spectra were recorded in fluorescence mode. Negligible changes in the line-shape and peak position of Pd K-edge XANES spectra were observed between two scans taken for a specific sample. The XAFS spectra of these standard samples (Pd-foil and PdO) were recorded in transmission mode. The spectra were processed and analyzed by the software codes Athena and Artemis. The conversion and enantiomeric excess were determined by HPLC analysis.

3. Methods for sample preparation

The catalyst was added to pre-cooled 2.5% glutaraldehyde in 1.5 mL centrifuge tubes and fixed at 4 °C for 12-24 h, then washed three times using PBS. It was dehydrated using a gradient of 30%, 50%, 70%, 80%, and 95% acetone (15 min each), followed by two 20-minute treatments with 100% acetone. The catalyst was sonicated, homogenized, and then placed on copper mesh for TEM and spherical aberration electron microscopy characterization. Transmission electron microscopy of biological sections was further embedded and sectioned. Other characterizations (ICP-OES、XRD、XPS、FT-IR etc.) were made directly using lyophilized catalyst powders.

4. Enzyme expression

The gene encoding of the alcohol dehydrogenase (ADHa)/amine dehydrogenase (AmDH)/monoamine oxidase (MAO) were inserted into expressing vector pET-28a (+), and the recombinant plasmids were transformed into *E. coli* BL21 (DE3) as the host organism for heterologous expression. Recombinant *E. coli* BL21 (DE3) strain was cultured in 10 mL LB media containing 50 μg/mL ampicillin (final concentration) at 37 °C and 180 rpm overnight. Next, 0.5 mL preculture was inoculated into a shake flask containing 50 mL TB media with 50 μg/mL ampicillin, cultured at 37 °C and 180 rpm until the optical density (OD_{600}) reached 0.6-0.8. The expression of the enzyme was induced by the addition of 0.5 mM IPTG (final concentration) and performed at 24 h at 20 °C. Then, the cells were harvested by centrifugation (5000 rpm, 4 °C, 10 min) and washed several times with precooling potassium phosphate buffer (50 mM, pH 7.5).

5. Preparation of SA-Pd_x@cell-ADHa

SA-Pd_x@cell-ADHa were synthesized by biodeposition and *in-situ* reduction of sodium tetrachloropalladate on cells. Cells (cell-ADHa, 20 mg/mL) were fully resuspended in PBS (50 mM, pH 7.5), then Na_2PdCl_4 (0.06/0.125/0.25/0.5/1/1.5/2/2.5/3/3.5/4 mM) aqueous solution was added and the mixture was shaken in a water bath shaker (180 rpm, 30 °C) for 3 h. Then, an appropriate amount of $NaBH_4$ was added for 2 min of reduction. Subsequently,

SA-Pd_x@cell-ADHa was obtained by centrifugation (7500 rpm, 4 °C, 5 min) and washed three times with pre-cooled PBS, stored at -20 °C.

6. Preparation of Si_t@SA-Pd_x@cell-ADHa

The silica coated SA-Pd_x@cell-ADHa catalysts (Si_t@SA-Pd_x@cell-ADHa) were prepared as follows: Firstly, SA-Pd_x@cell-ADHa (2 g) was resuspend sufficiently in 100 mL PBS buffer solution (50 mM, pH=7.5). Subsequently, Tetraethyl orthosilicate (TEOS) (90 mM) was added and hydrolyzed for 20 min before slow dropwise addition of 3-aminopropyltriethoxysilane (APTES) (11.25/ 22.5/45/90 mM). The mixture continued to be shaken at 30 °C for 1 h. Then, Si_t@SA-Pd_x@cell-ADHa was harvested by centrifugation (7500 rpm, 4 °C, 5 min) and washed three times with pre-cooled PBS, stored at -20 °C.

7. Procedure for C=O bond reduction over SA-Pd_x@cell-ADHa

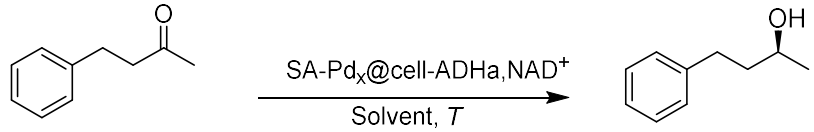

The benzylacetone (50 mM) was dissolved in 2 mL PBS buffer (50 mM, pH 7.5) containing 100 mg SA-Pd_x@cell-ADHa, NAD^+ (15 mM), *i*-PrOH (15%, v/v). The reaction mixture was shaken at a 40 °C incubator for 2 h. After the reaction finished, the solution was extracted using hexane (3 × 10 mL). The products were determined by HPLC analysis.

8. Procedure for the fully asymmetric reduction of enones over SA-Pd_x@cell-ADHa

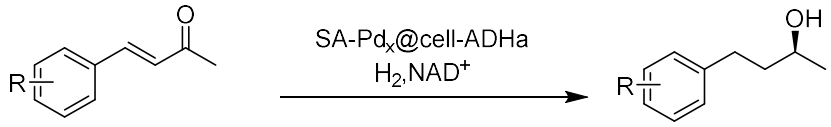

The reaction was conducted in a dry Schlenk tubes, the corresponding enones (50 mM/10 mM) was dissolved in 2 mL PBS buffer (50 mM, pH 7.5) containing 100 mg SA-Pd_x@cell-ADHa, NAD^+ (15 mM), *i*-PrOH (15%, v/v).The reaction mixture was stirred at 40 °C for 2 h under the hydrogen atmosphere. After the reaction finished, the solid catalyst was recovered by centrifugation, while the filtrate was extracted with hexane (3 × 10 mL). The products were determined by HPLC or GC analysis.

9. Procedure for the synthesis of racemic alcohols

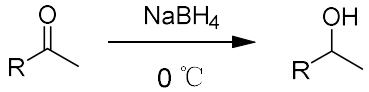

A solution of corresponding ketone (100 mM) was first cooled in ethanol to 0 °C. Solid $NaBH_4$ (120 mM) was then added to the reaction mixture over the course of 1 h. The suspension was stirred at 0 °C for an additional hour. To quench the excess $NaBH_4$, a saturated aqueous solution of NH_4Cl was added dropwise. Once the quenching was complete, the mixture was poured into a separatory funnel containing water (100 mL). The organic phase was extracted with dichloromethane (CH_2Cl_2, 3 × 30 mL). The combined organic layers were washed with brine (50 mL), and then dried over $MgSO_4$. After filtering the combined organic layers, the solvent was removed under reduced pressure. Finally, the crude reaction mixture was purified by column chromatography on silica gel, using mixture of hexane and EtOAc (80:20) as the eluent.

10. Procedure for stability tests

Thermal stability test: The catalysts Si_{76}@SA-$Pd_{0.97}$@cell-ADHa, SA-$Pd_{0.97}$@cell-ADHa and Pd/C +free cell-ADHa system were incubated at 70 °C for a certain period of time, and an appropriate amount of them was taken out after an interval of 6 h, which was used in the general procedure for fully asymmetric reduction of enones, and the relative catalytic activities with the initial catalysts were detected.

pH stability test: Si_{76}@SA-$Pd_{0.97}$@cell-ADHa, SA-$Pd_{0.97}$@cell-ADHa and Pd/C catalysts +free cell-ADHa system were incubated in buffer solutions at pH 5 and pH 11 for a certain period of time, and an appropriate amount of the catalysts was removed after a certain time interval to be used in the general procedure for the fully asymmetric reduction of ketene and examined for the catalytic activity in comparison with that of the initial catalysts. catalytic activity with respect to the initial catalyst.

Mechanical stability test: Si_{76}@SA-$Pd_{0.97}$@cell-ADHa, SA-$Pd_{0.97}$@cell-ADHa and Pd/C catalysts +free cell-ADHa were stirred vigorously at 1800 rpm for a period of time, and equal amounts of the catalysts were removed at intervals to be used in a general procedure for the fully asymmetric reduction of enones and tested for their relative catalytic activity compared to that of the initial catalyst. catalytic activity with respect to the initial catalyst.

Storage stability test: Si_{76}@SA-$Pd_{0.97}$@cell-ADHa, SA-$Pd_{0.97}$@cell-ADHa were stored at -20 °C, and equal amounts of the catalysts were removed at intervals to be used in the general procedure for the fully asymmetric reduction of alkenones and tested for their relative catalytic activity to that of the initial catalysts.

11. Procedure for reusability test

Trans-benzylideneacetone (50 mmol), catalyst, isopropanol (15%, v/v), NAD^+, and PBS (1.7 mL) were added to a dry Schlenk tube and the reaction mixture was stirred at a temperature of 40 °C under a hydrogen atmosphere for 2 h. Upon completion of the reaction, the catalyst was recovered by centrifugation and washed twice with PBS to proceed to the next cycle. The supernatant was extracted using hexane and the relative activity of the catalyst after each cycle was detected by liquid chromatography.

12. The synthesis of chiral amines from enones catalyzed by SA-Pd@cell-AmDH

The reaction was carried out in a dry Schlenk tube by dissolving trans-benzylideneacetone in 2 mL of $NH_4Cl/NH_3{\cdot}H_2O$ buffer (2 M, pH = 10) containing 100 mg of SA-Pd@cell-ADHa, NAD^+ (0.4% eq.), GDH, and glucose, and stirred the mixture for 2 h at 40 °C under hydrogen gas. After the reaction finished, the solid catalyst was recovered by centrifugation and the filtrate was extracted with ethyl acetate (3 × 10 mL). The products were quantitatively analyzed by GC analysis.

13. Deracemisation progress of 1-phenyl-1,2,3,4-tetrahydroisoquinoline by SA-Pd@cell-MAO

1-phenyl-1,2,3,4-tetrahydroisoquinoline (PTQ) (10 mM), SA-Pd@cell-MAO were added to a 25 mL Schlenk tube containing 4.5 mL of PBS (100 mM, pH=7.5) and 0.5 mL of iso-octane, and the oxidation process was carried out in an open-mouth reaction for 6 h at 35 °C. The air in the reaction vials was then expelled by a vacuum pump, and a balloon was connected to provide hydrogen gas for the reaction. The reduction process was carried out at 35 °C for 6 h. The oxidation and reduction processes were repeated five times. The reaction was centrifuged and extracted with the supernatant of methyl tert-butyl ether, and the yields and ee values were determined by HPLC analysis.

14. Preparation of SA-Au@cell and the catalytic reduction of *p*-nitrophenol

SA-Au@cell were synthesized by biodeposition and in-situ reduction of sodium tetrachloropalladate on cells. Cells were fully resuspended in PBS (50 mM, pH 7.5), then $HAuCl_4$ aqueous solution (1 mM) was added and the mixture was shaken in a water bath shaker (180 rpm, 30 °C) for 3 h. Then, an appropriate amount of $NaBH_4$ was added for 2 min of reduction. Subsequently, SA-Au@cel was obtained by centrifugation (7500 rpm, 4 °C, 5 min) and washed three times with pre-cooled PBS. Then, kinetic experiments for the reduction of *p*-nitrophenol (*p*-NP) were conducted in a 4 mL quartz cuvette using a UV–vis spectrophotometer. In brief, 200 mg of SA-Au@cell, 2.7 mL of water, 100 μL of 0.2 M *p*-NP, and newly prepared 150 μL of $NaBH_4$ (0.1 M) were mixed in the 4 mL quartz cuvette. The progress of the reaction was monitored by tracking the change in *p*-NP peak intensity at 400 nm over time.

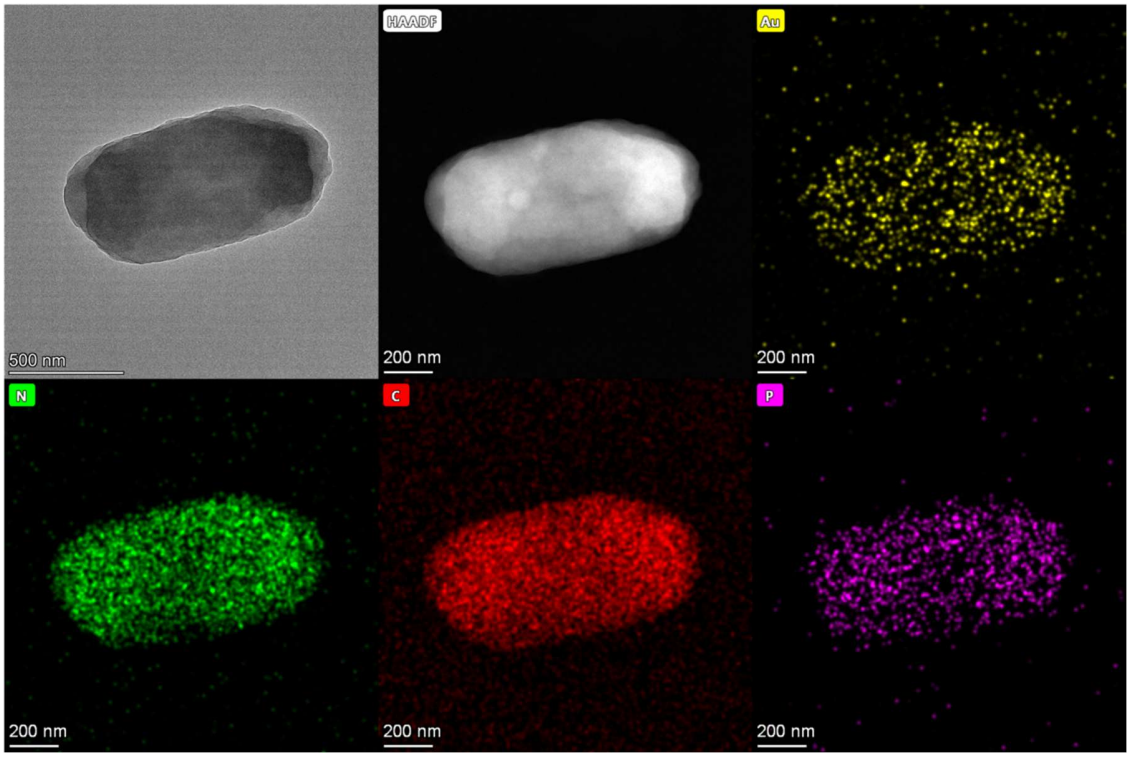

Figure S1. STEM, HAADF-STEM and elemental mapping images for the SA-$Au_{2.72}$@cell catalyst.

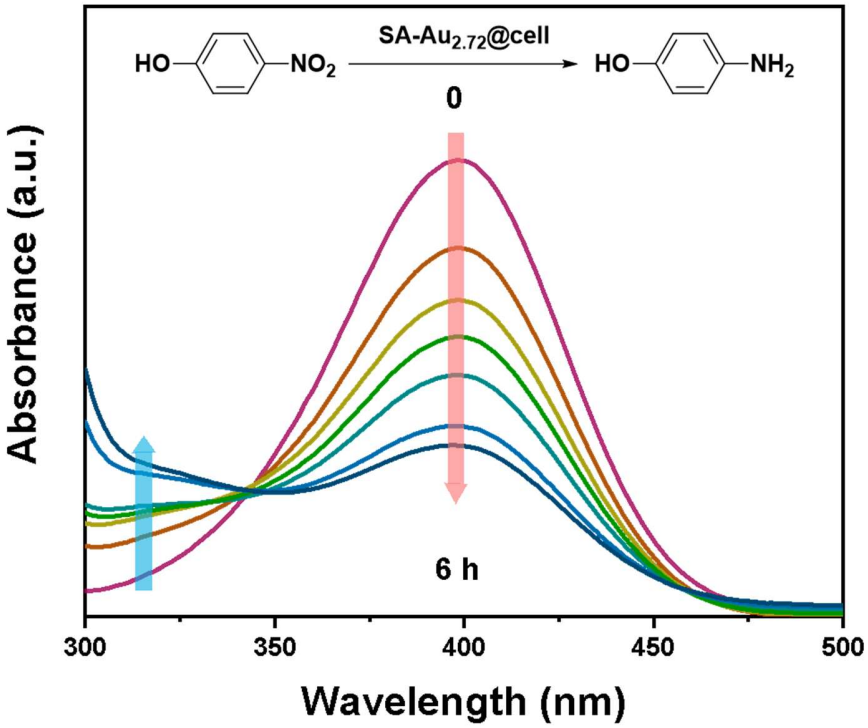

Figure S2. UV spertrum of SA-$Au_{2.72}$@cell catalyzing the formation of *p*-aminophenol from *p*-nitrophenol.

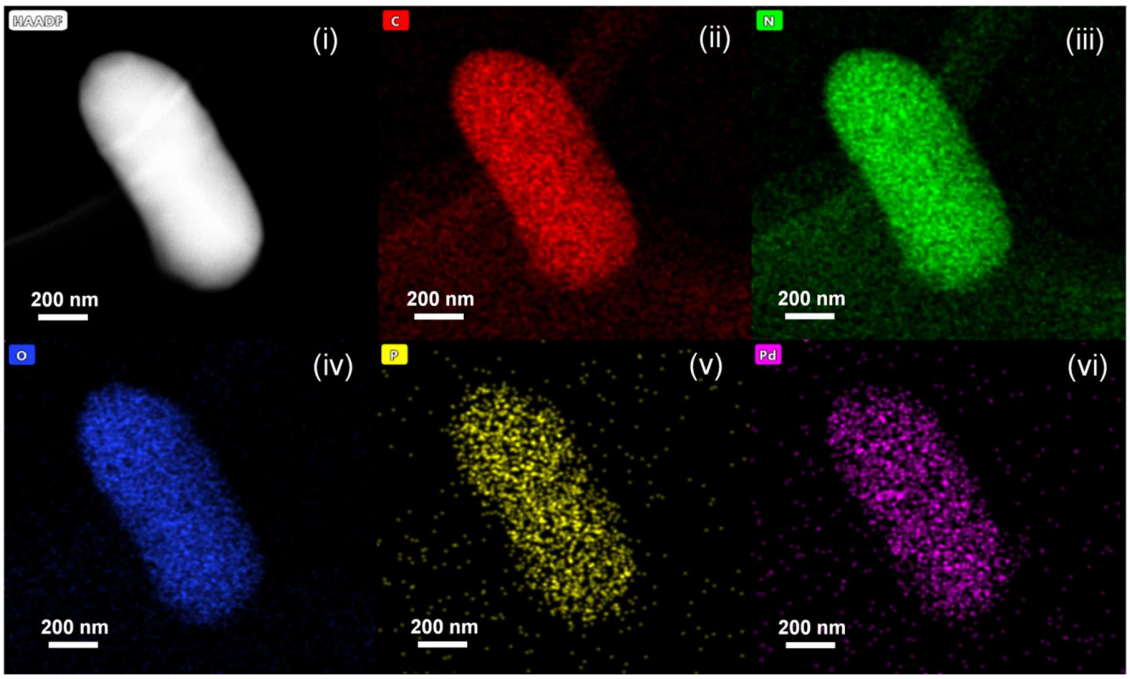

Figure S3. The HAADF-STEM image (i) and the elemental mapping images (ii-vi) of SA-$Pd_{0.97}$@cell-ADHa.

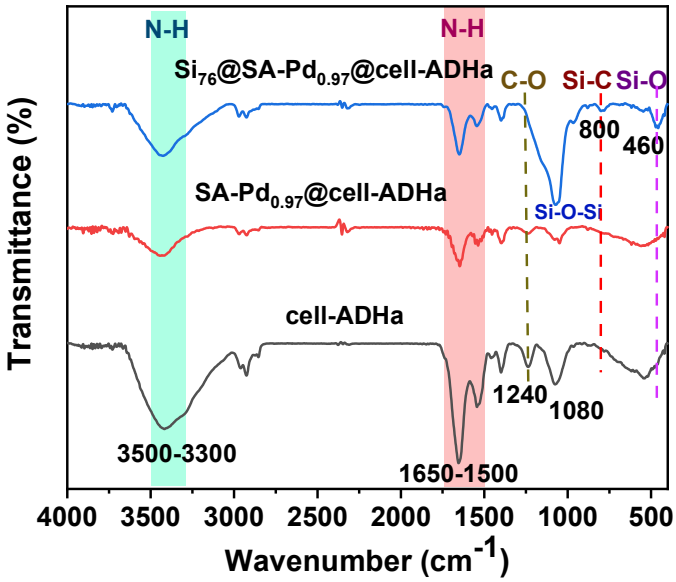

Figure S4. The FT-IR spectra of cell-ADHa, SA-$Pd_{0.97}$@cell-ADHa and Si_{76}@SA-$Pd_{0.97}$@cell-ADHa.

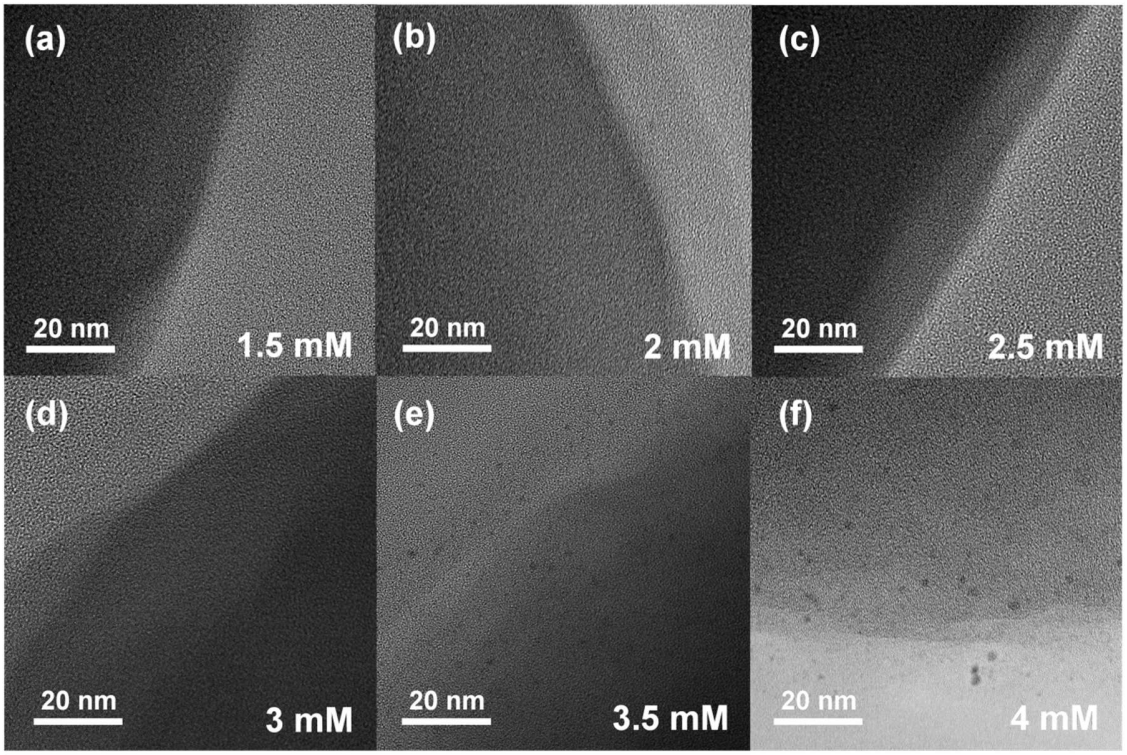

Figure S5. STEM images for the integrated catalysts prepared using various concentrations of Na_2PdCl_4.

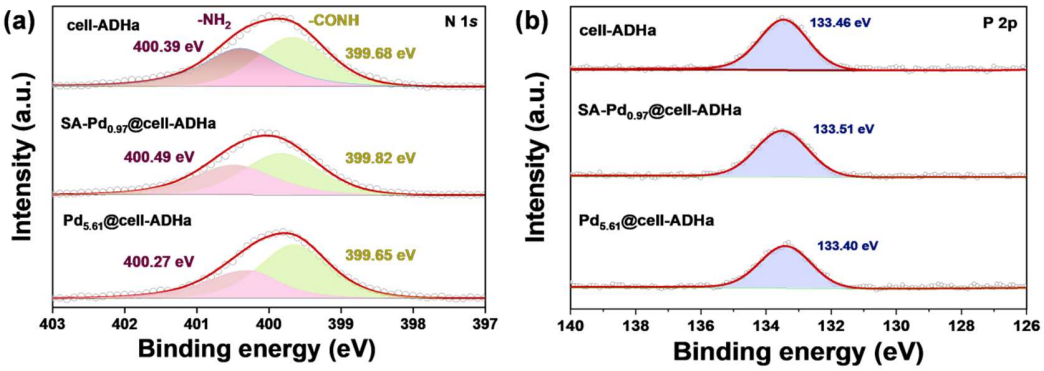

Figure S6. High-resolution (a) N1s and (b) P2p XPS spectra of cell-ADHa, SA-$Pd_{0.97}$@cell-ADHa and $Pd_{5.61}$@cell-ADHa.

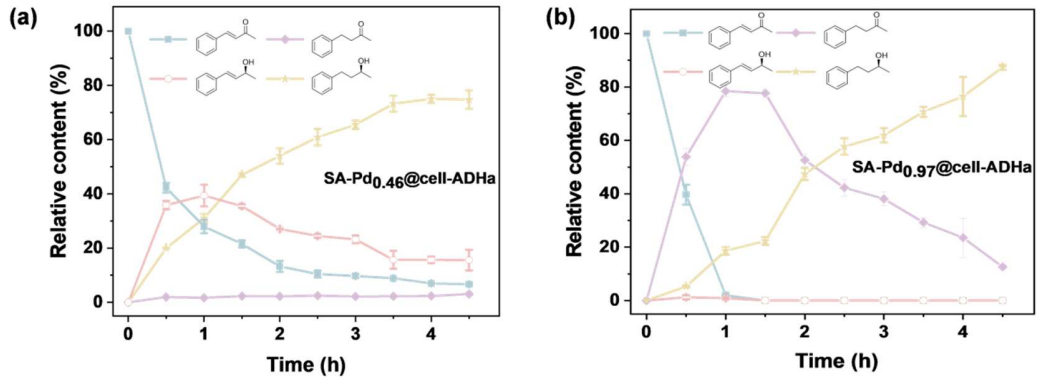

Figure S7. Reaction process curves for the (a) SA-$Pd_{0.46}$@cell-ADHa and (b) SA-$Pd_{0.97}$@cell-ADHa.

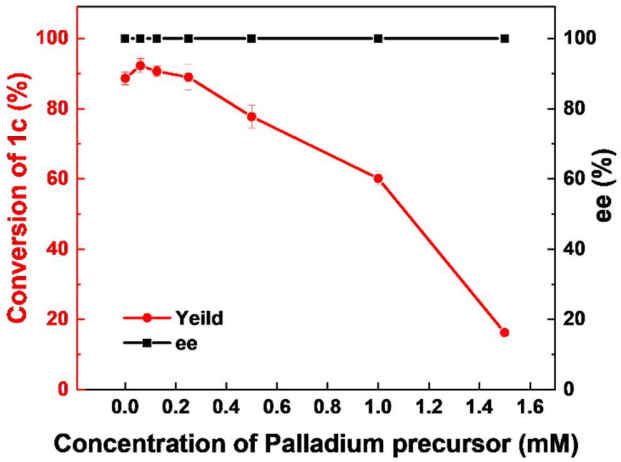

Figure S8. The effect of palladium precursor incorporation concentration on the biocatalytic activity of catalysts.

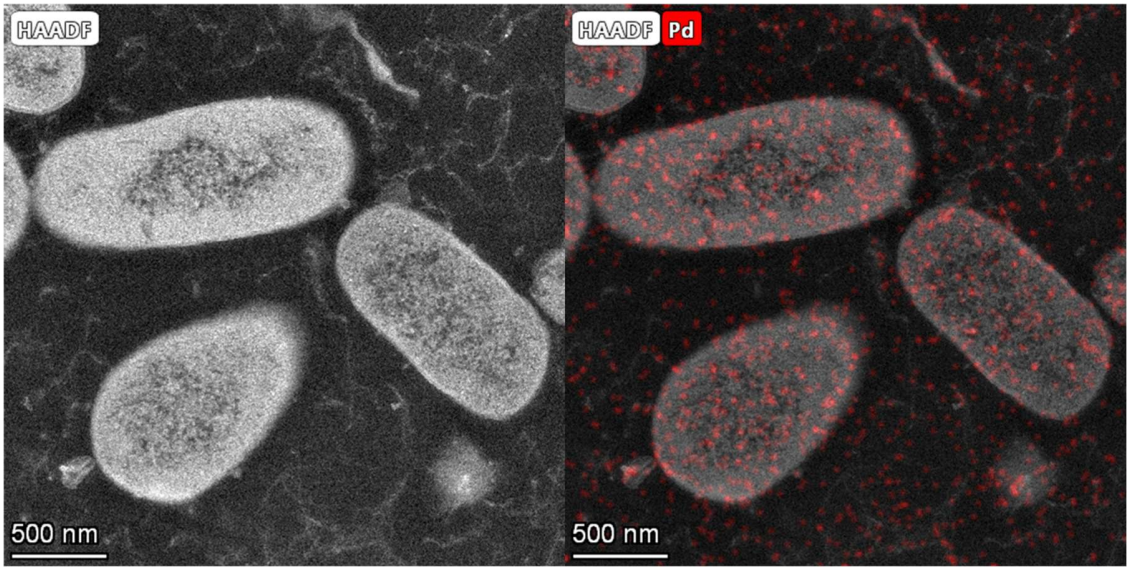

Figure S9. The biological transmission electron microscope (Bio-TEM) and elemental mapping images for the SA-$Pd_{0.56}$@cell-ADHa cross-section.

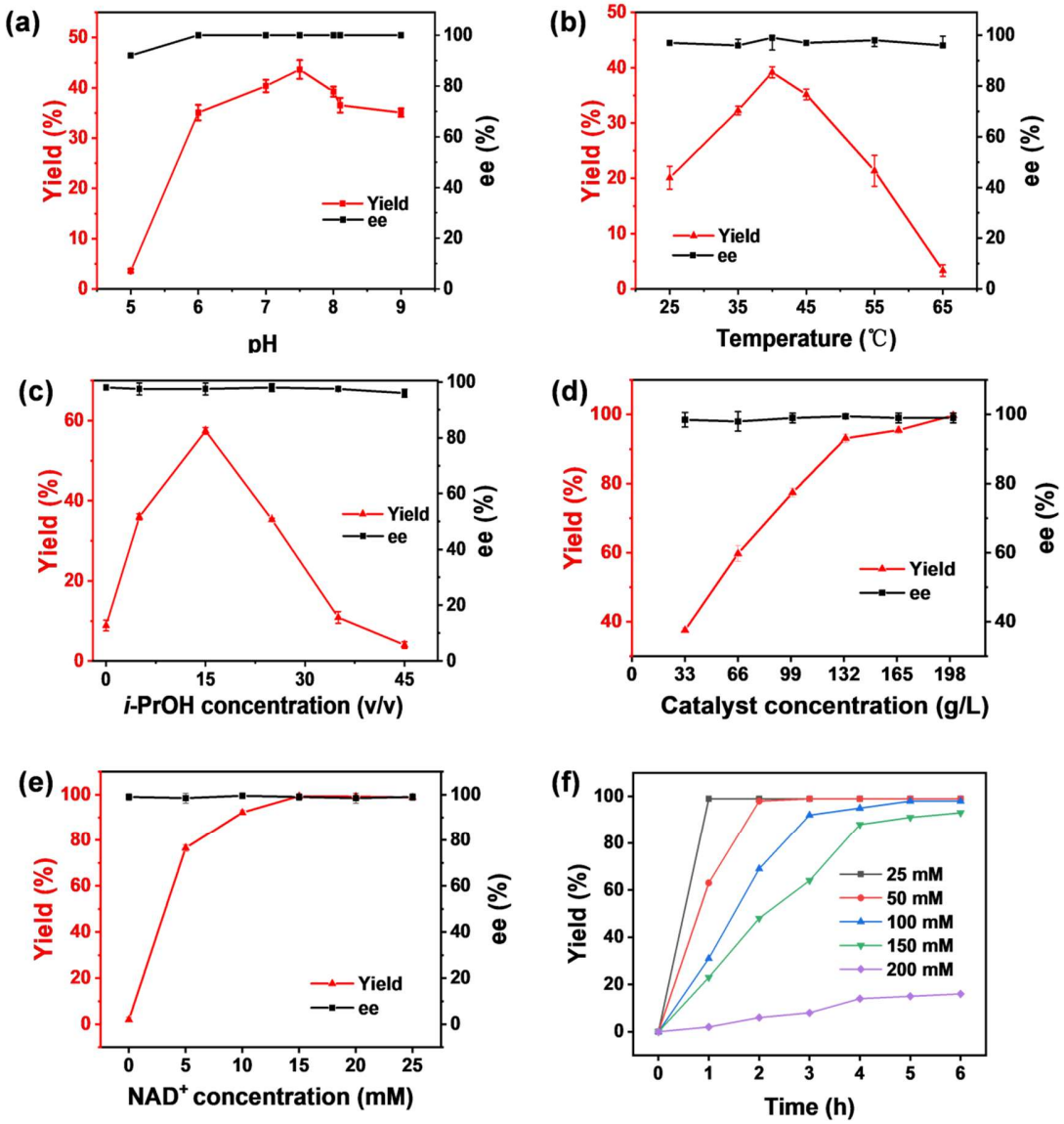

Figure S10. The optimization of reaction conditions for one-pot cascade catalyzed enone hydrogenation of SA-$Pd_{0.97}$@cell-ADHa.

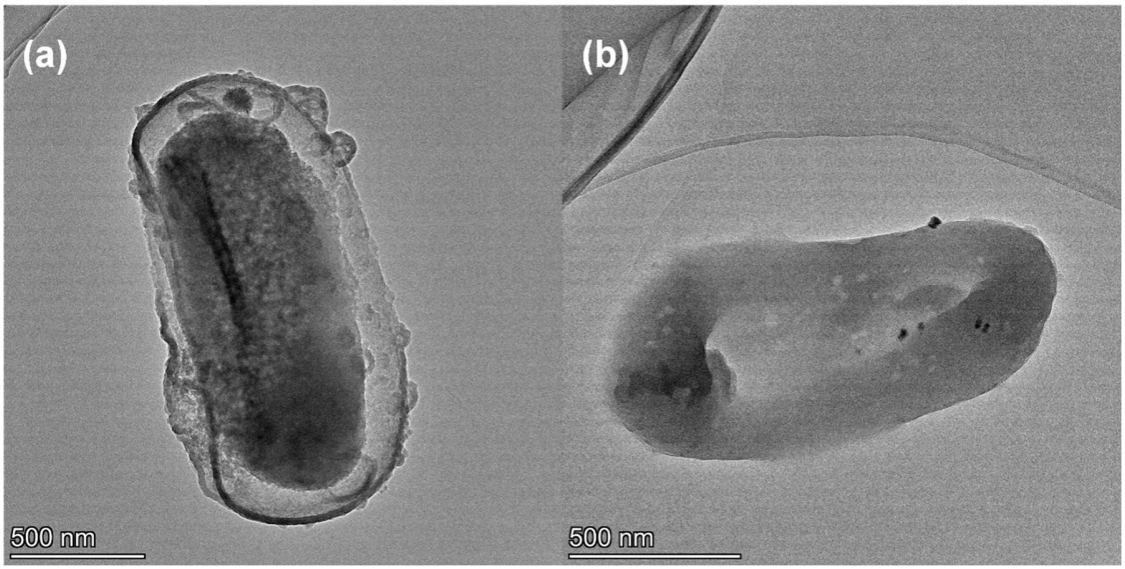

Figure S11. The TEM images of the (a) Si_{76}@SA-$Pd_{0.97}$@cell-ADHa after 18 cycles and (b) SA-$Pd_{0.97}$@cell-ADHa after 6 cycles.

Table S1. Palladium content of catalysts.

Addition of Na_2PdCl_4 (mM)	Pd content (wt%)	Catalysts name
0.0625	0.06	SA-$Pd_{0.06}$@cell-ADHa
0.125	0.18	SA-$Pd_{0.18}$@cell-ADHa
0.25	0.46	SA-$Pd_{0.46}$@cell-ADHa
0.5	0.74	SA-$Pd_{0.74}$@cell-ADHa
1	0.97	SA-$Pd_{0.97}$@cell-ADHa
1.25	1.54	SA-$Pd_{1.54}$@cell-ADHa
1.5	2.46	SA-$Pd_{2.46}$@cell-ADHa
2	2.96	SA-$Pd_{2.96}$@cell-ADHa
2.5	3.57	SA-$Pd_{3.57}$@cell-ADHa
3	4.12	SA-$Pd_{4.12}$@cell-ADHa
3.5	4.98	$Pd_{4.98}$@cell-ADHa
4	5.61	$Pd_{5.61}$@cell-ADHa

Table S2. Performances of various single atom Pd catalyst preparation.

SAC Catalyst	Carrier	Precursor	Temperature [℃]	Pd [wt%]	Ref
SA-Pd@cell-ADHa	*E.coli* cell	Na_2PdCl_4	r.t.	4.12	This work
Pd1/ND@G	ND@G	$Pd(NO)_3$	100	0.11	[1]
Pd/MVF	MVF	$PdCl_2$	60	1.11	[2]
Pd/TiO_2	TiO_2	H_2PdCl_4	350	0.0475	[3]
Pd/TiO_2-anatase	TiO_2-anatase	$Pd(NH_3)_4(NO_3)_2$	400	0.0125	[4]
$Pd1/TiO_2$(EG–stabilized)	TiO_2	H_2PdCl_4	r.t.	1.5	[5]
Pd-NC	NC	H_2PdCl_4	900	2.95	[6]
1Pd/ceria-800*	Calcined-CeO_2	$H_8N_5O_3Pd^+$	800	1	[7]
Pd1/N-graphene	Nitrogen-doped graphene	Na_2PdCl_4	800	2.91	[8]
$Pd_{0.033}/TP\text{-}TTA/SiO_2$	TP-TTA/SiO_2	$Pd(CH_3CN)_2Cl_2$	200	0.033	[9]
$Pd1/NOC/Al_2O_3$	NOC/Al_2O_3	Na_2PdCl_4	400	0.41	[10]
$Pd\text{-}SAs/3DOM\text{-}CeO_2$	3DOM-CeO_2	$(NH_4)_2PdCl_4$	450	1.76	[11]
$Pd_1/\alpha\text{-}MoC$	α-MoC	$Pd(NO_3)_2$	700	5	[12]
Pd_1/CALB-P	enzyme–pluronic conjugate	$PdCl_2$	r.t.	4.0	[13]
SA-Pd@GS	*G. sulfurreducens*	$PdNO_3{\cdot}2H_2O$	30	0.2	[14]

Table S3. EXAFS fitting parameters at the Pd K-edge for various samples.

Sample	shell	*C*N$^{\alpha}$	R(Å)^{b}	σ^2(Å^2)^{c}	ΔE_0(eV)^{d}	*R*factor
Pd foil	Pd-Pd	12*	2.733±0.002	0.0051±0.0002	1.7±0.3	0.0021
PdO	Pd-O	4.2±0.3	2.071±0.002	0.0010±0.0008	4.3±0.5	0.0057
	Pd-Pd	3.6±0.5	3.022±0.001	0.0034±0.0008	-1.1±0.4	
	Pd-Pd	8.2±1.2	3.413±0.001			
SA-$Pd_{0.97}$@cell-ADHa	Pd-O	3.5±0.4	2.044±0.012	0.0029±0.0016	3.7±1.6	0.0111

N is the coordination number; *R* is interatomic distance; σ^2 is Debye-Waller factor; ΔE_0 is edge-energy shift; R factor is a measure of the goodness of the fitting. Error bounds that characterize the structural parameters obtained by EXAFS spectroscopy were estimated as N±20%; R±1%; σ^2±20%; ΔE_0±20%.

NMR data

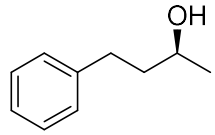

^{1}H NMR (600 MHz, DMSO-d_6) δ 7.26 (t, J = 7.7 Hz, 2H), 7.21 – 7.17 (m, 2H), 7.15 (td, J = 7.3, 1.4 Hz, 1H), 4.45 (d, J = 4.8 Hz, 1H), 3.59 (dh, J = 11.2, 5.9 Hz, 1H), 2.61 (dddd, J = 56.1, 13.6, 9.6, 6.4 Hz, 2H), 1.66 – 1.54 (m, 2H), 1.08 (d, J = 6.1 Hz, 3H). ^{13}C NMR (151 MHz, DMSO-d_6) δ 142.94, 128.70, 128.68, 125.96, 65.70, 41.36, 32.06, 24.07. HPLC conditions: CHIRALCEL®OD-H (cellulose tris(3,5-dimethylphenylcarbamate) coated on silica gel); mobile phase, n-hexane/ isopropyl alcohol (99/5); flow rate, 1 mL/min; column temperature 30 °C.

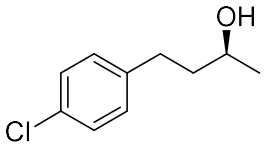

^{1}H NMR (400 MHz, Chloroform-d) δ 7.25 (d, J = 1.9 Hz, 1H), 7.23 (d, J = 1.7 Hz, 1H), 7.16 – 7.13 (m, 1H), 7.12 (s, 1H), 3.81 (q, J = 6.3 Hz, 1H), 2.68 (ddq, J = 30.2, 14.4, 8.0 Hz, 2H), 1.73 (ddd, J = 14.5, 9.3, 3.2 Hz, 2H), 1.42 (s, 1H), 1.22 (dd, J = 6.2, 1.6 Hz, 3H). ^{13}C NMR (101 MHz, Chloroform-d) δ 140.53, 131.52, 129.77, 128.49, 67.32, 40.69, 31.46, 23.72. HPLC conditions: CHIRALCEL®OD-H (cellulose tris(3,5-dimethylphenylcarbamate) coated on silica gel); mobile phase, n-hexane/ isopropyl alcohol (99/1); flow rate, 1 mL/min; column temperature 30 °C.

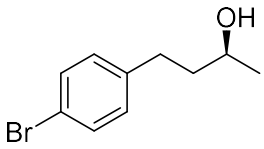

^{1}H NMR (400 MHz, Chloroform-d) δ 7.40 (dd, J = 8.2, 1.7 Hz, 2H), 7.11 – 7.04 (m, 2H), 3.81 (h, J = 6.4 Hz, 1H), 2.66 (ddt, J = 30.2, 13.3, 7.7 Hz, 2H), 1.79 – 1.69 (m, 2H), 1.23 (dd, J = 6.2, 1.5 Hz, 3H). 13C NMR (101 MHz, Chloroform-d) δ 141.04, 131.43, 130.19, 119.52, 67.31, 40.62, 31.52, 23.74. HPLC conditions: CHIRALCEL®OD-H (cellulose tris(3,5-dimethylphenylcarbamate) coated on silica gel); mobile phase, n-hexane/ isopropyl alcohol (99/1); flow rate, 1 mL/min; column temperature 30 °C.

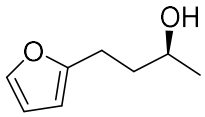

^{1}H NMR (400 MHz, Chloroform-*d*) δ 7.24 (s, 1H), 6.22 (s, 1H), 5.94 (d, *J* = 3.2 Hz, 1H), 3.77 (q, *J* = 6.3 Hz, 1H), 2.70 (d, *J* = 7.7 Hz, 1H), 2.66 (d, *J* = 8.0 Hz, 1H), 1.72 (q, *J* = 7.9 Hz, 2H), 1.41 (s, 1H), 1.16 (d, *J* = 6.2 Hz, 3H). ^{13}C NMR (101 MHz, Chloroform-d) δ 155.79, 140.93, 110.15, 104.90, 67.35, 37.37, 24.35, 23.51. HPLC conditions: CHIRALCEL®OD-H (cellulose tris(3,5-dimethylphenylcarbamate) coated on silica gel); mobile phase, n-hexane/ isopropyl alcohol (99/1); flow rate, 1 mL/min; column temperature 30 °C.

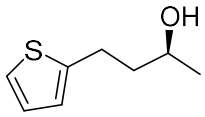

^{1}H NMR (400 MHz, Chloroform-*d*) δ 7.14 (dd, *J* = 5.1, 1.2 Hz, 1H), 6.94 (dd, *J* = 5.1, 3.4 Hz, 1H), 6.84 (dd, *J* = 3.4, 1.0 Hz, 1H), 3.89 (h, *J* = 6.2 Hz, 1H), 2.97 (tq, *J* = 16.0, 8.2, 7.7 Hz, 2H), 1.94 – 1.79 (m, 2H), 1.26 (d, *J* = 6.2 Hz, 3H). ^{13}C NMR (101 MHz, Chloroform-*d*) δ 144.92, 126.79, 124.24, 123.05, 67.24, 41.00, 26.23, 23.69, 23.62. HPLC conditions: CHIRALCEL®OD-H (cellulose tris(3,5-dimethylphenylcarbamate) coated on silica gel); mobile phase, n-hexane/ isopropyl alcohol (99/1); flow rate, 1 mL/min; column temperature 30 °C.

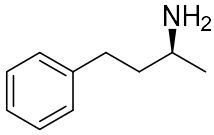

^{1}H NMR (600 MHz, DMSO-d_6) δ 7.26 (t, *J* = 7.6 Hz, 2H), 7.21 – 7.18 (m, 2H), 7.15 (t, *J* = 7.3 Hz, 1H), 2.73 (q, *J* = 6.3 Hz, 1H), 2.65 – 2.55 (m, 2H), 1.51 (dtd, *J* = 9.3, 6.8, 3.3 Hz, 3H), 0.99 (d, *J* = 6.3 Hz, 3H). ^{13}C NMR (151 MHz, DMSO-d_6) δ 143.04, 128.68, 128.67, 125.95, 46.43, 42.22, 32.59, 24.60. GC conditions: Agilgent CP-Chirasil Dex CB (df = 0.25 μm, 0.32 mm i.d. × 25 m); carrier gas, N_2 (flow 30 mL/min); injection temp, 280 °C; initial column temperature 100 °C, then progress rate, 5 °C/min; final column temperature, 200 °C.

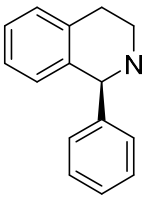

^{1}H NMR (600 MHz, DMSO-d_6) δ 7.30 (t, J = 7.5 Hz, 2H), 7.25 (d, J = 7.5 Hz, 3H), 7.15 – 7.10 (m, 1H), 7.09 (t, J = 7.3 Hz, 1H), 7.02 – 6.96 (m, 1H), 6.62 (d, J = 7.7 Hz, 1H), 4.97 (s, 1H), 3.12 – 3.06 (m, 1H), 2.95 – 2.86 (m, 2H), 2.81 – 2.68 (m, 2H). ^{13}C NMR (151 MHz, DMSO-d_6) δ 139.30, 129.32, 129.24, 128.47, 127.97, 127.27, 125.65, 39.57, 29.72. HPLC conditions: CHIRALPAK®AD (amylose tris(3,5-dimethylphenylcarbamate)coated on silica gel); mobile phase, n-hexane/ isopropyl alcohol (99/5); flow rate, 1 mL/min; column temperature 30 °C.

NMR spectras

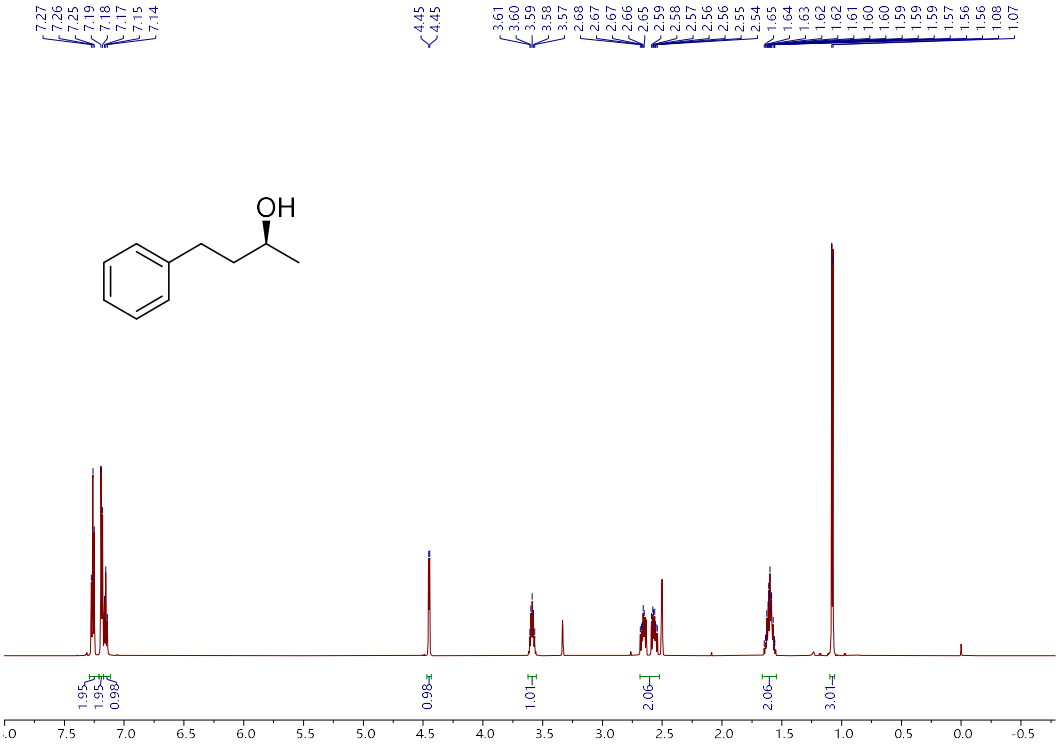

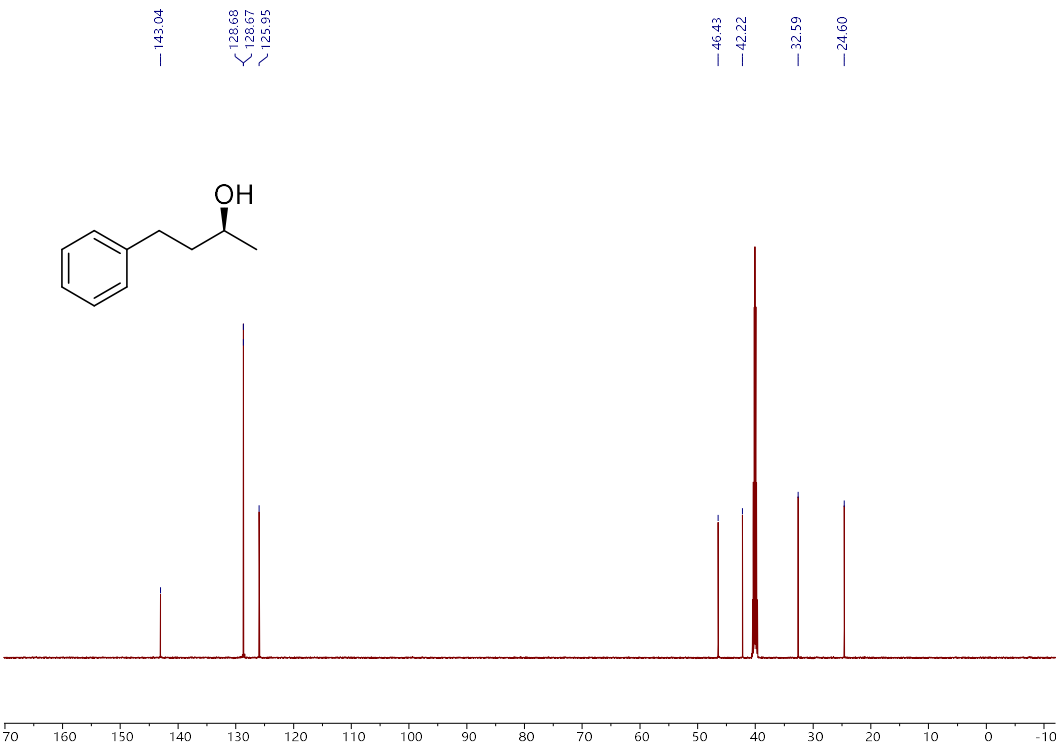

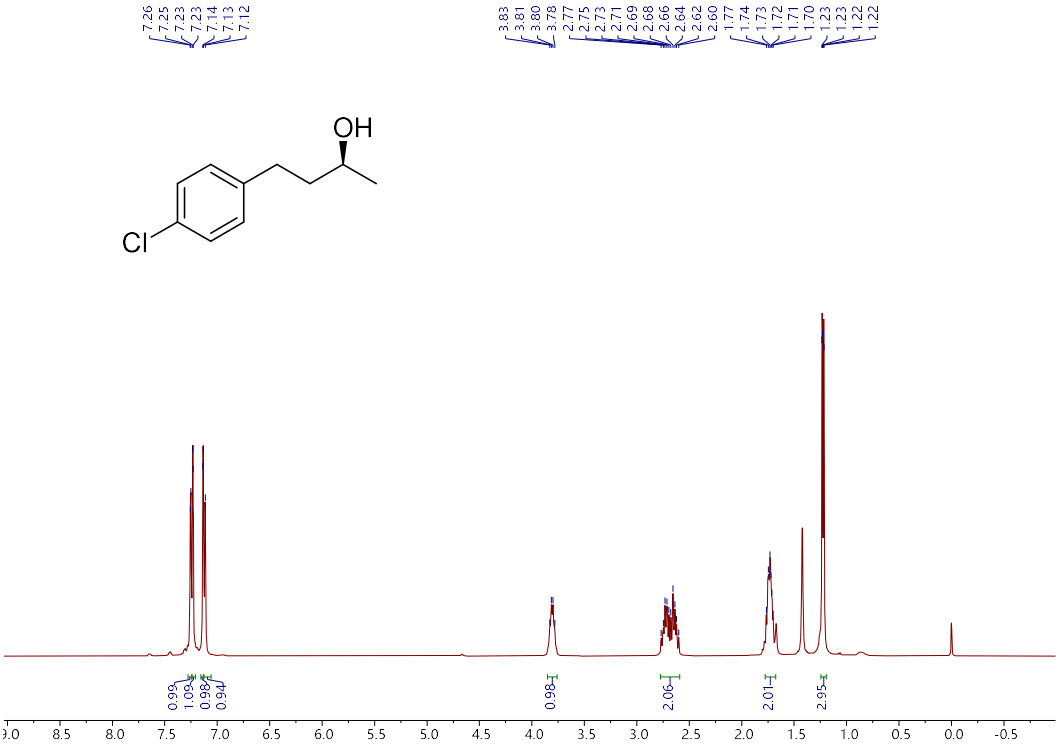
7.26
7.25
7.23
7.23
7.14
7.13
7.12
3.83
3.81
3.80
3.78
2.77
2.75
2.73
2.71
2.69
2.68
2.66
2.64
2.62
2.60
1.77
1.74
1.73
1.72
1.71
1.70
1.23
1.23
1.22
1.22
OH
Cl
0.99
1.09
0.96
0.94
0.98
2.06
2.01
2.95

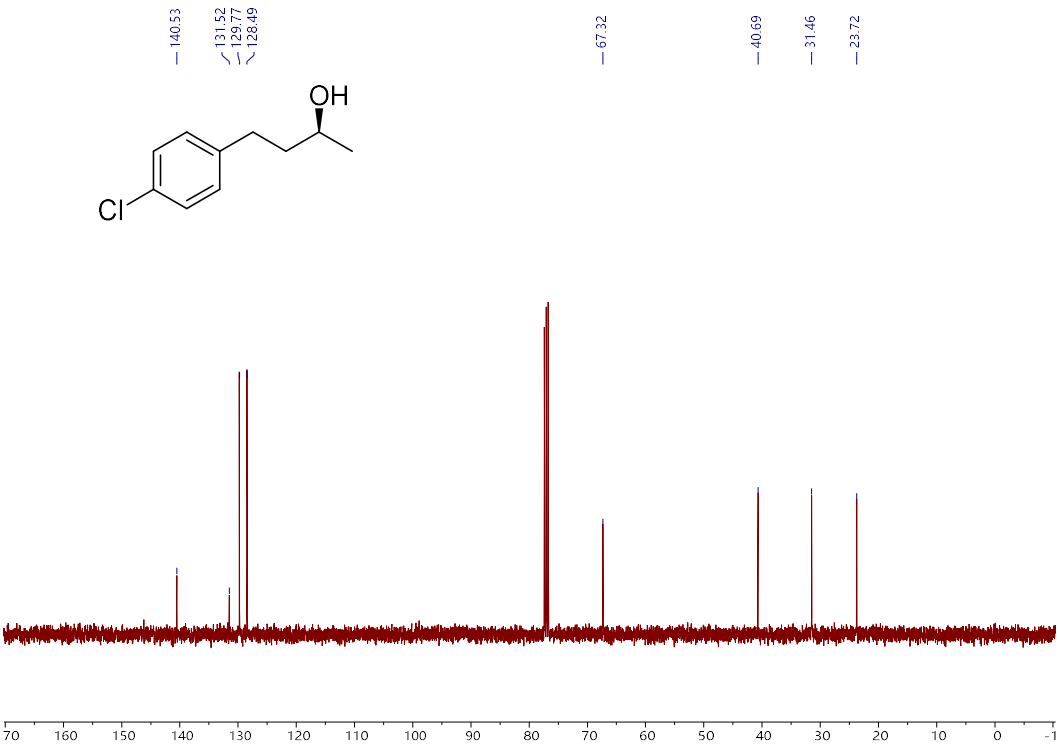
140.53
131.52
129.77
128.49
67.32
40.69
31.46
23.72
OH
Cl

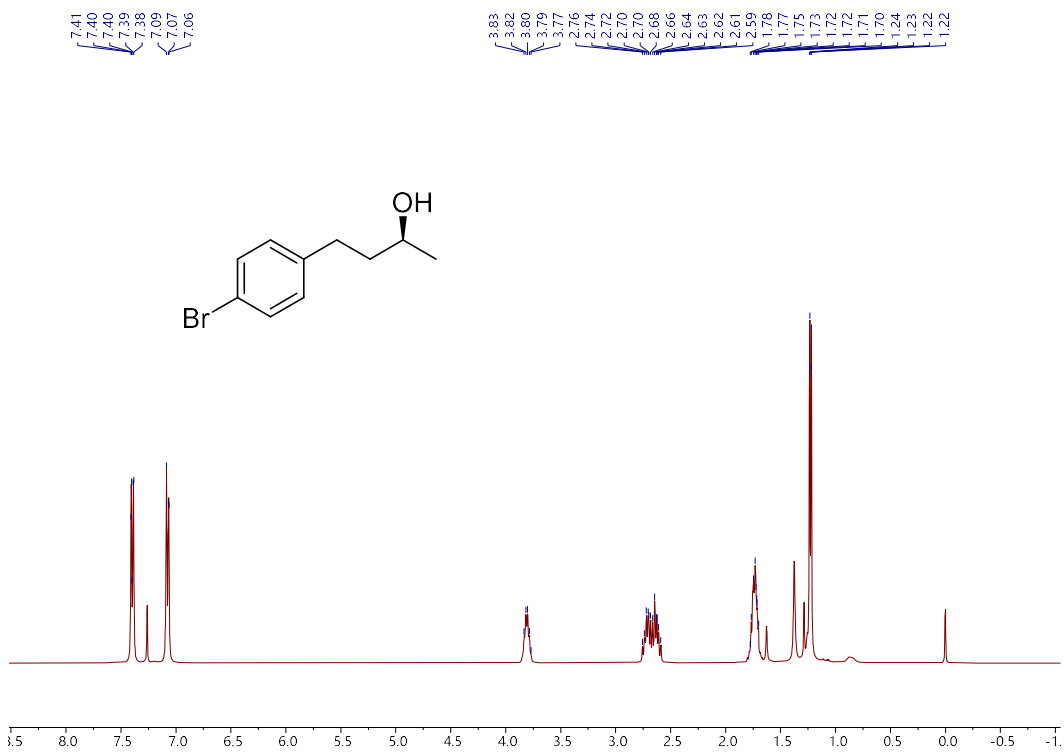
7.41
7.40
7.40
7.39
7.38
7.09
7.07
7.06
3.83
3.82
3.80
3.79
3.77
2.76
2.74
2.72
2.70
2.70
2.68
2.66
2.64
2.63
2.62
2.61
2.59
1.78
1.77
1.75
1.73
1.72
1.72
1.71
1.70
1.24
1.23
1.22
1.22
OH
Br
8.0
7.5
7.0
6.5
6.0
5.5
5.0
4.5
4.0
3.5
3.0
2.5
2.0
1.5
1.0
0.5
0.0
-0.5

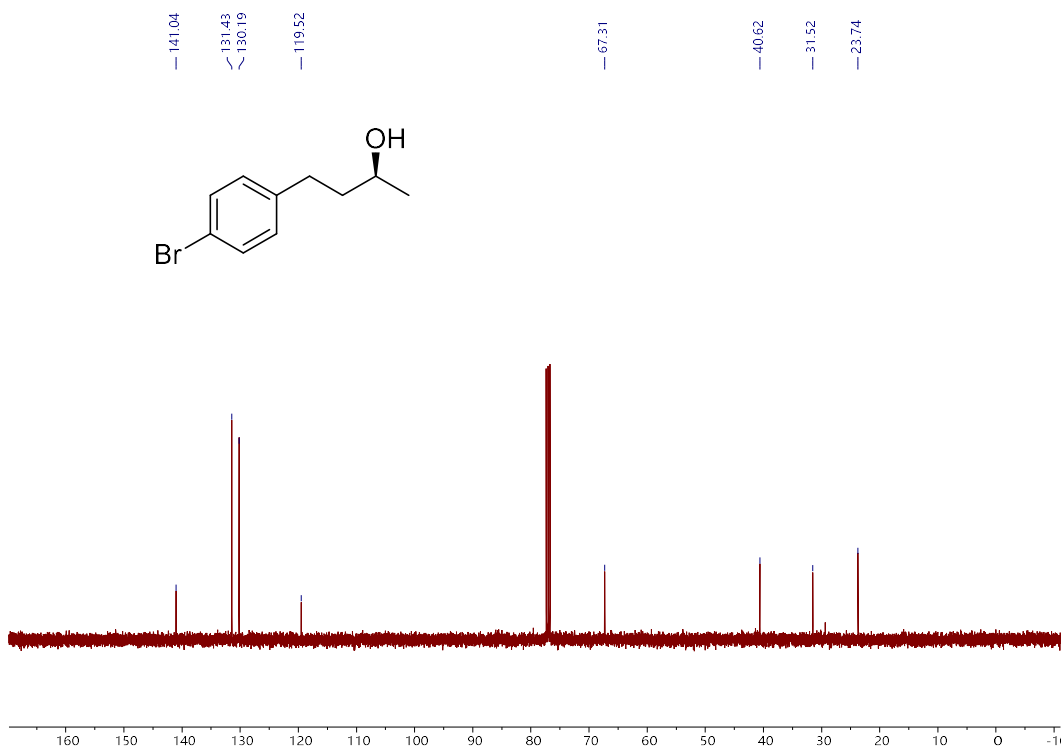
141.04
131.43
130.19
119.52
67.31
40.62
31.52
23.74
OH
Br
160
150
140
130
120
110
100
90
80
70
60
50
40
30
20
10
0

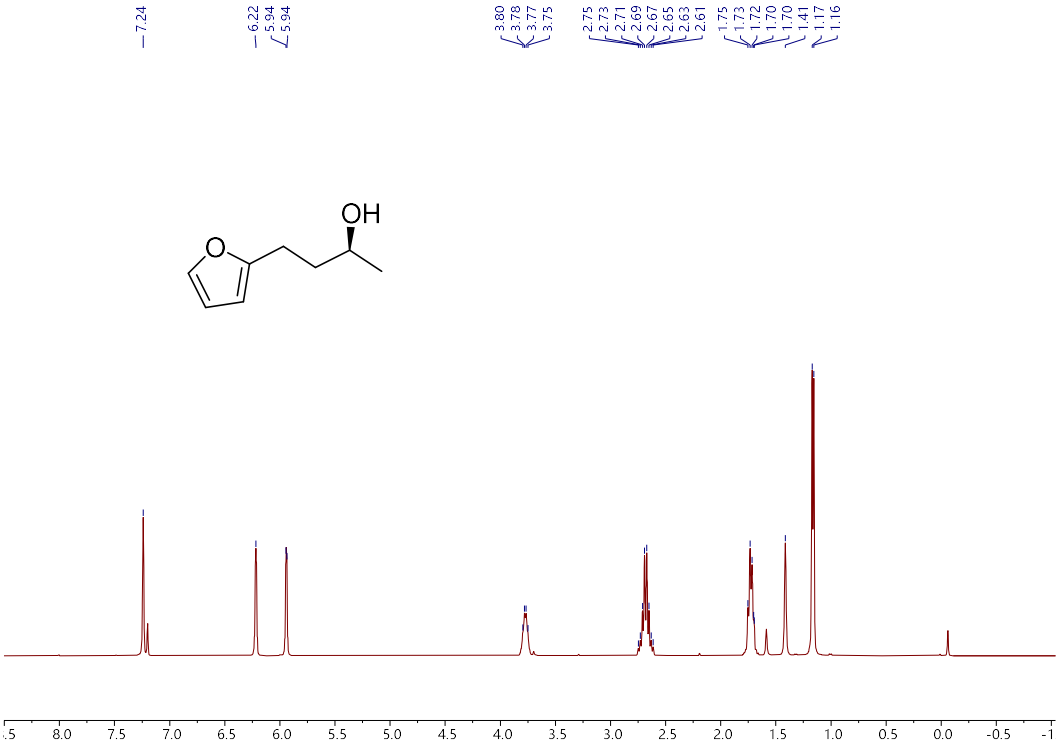
7.24
6.22
5.94
5.94
3.80
3.78
3.77
3.75
2.75
2.73
2.71
2.69
2.67
2.65
2.63
2.61
1.75
1.73
1.72
1.70
1.70
1.41
1.17
1.16
OH
O
8.0
7.5
7.0
6.5
6.0
5.5
5.0
4.5
4.0
3.5
3.0
2.5
2.0
1.5
1.0
0.5
0.0
-0.5

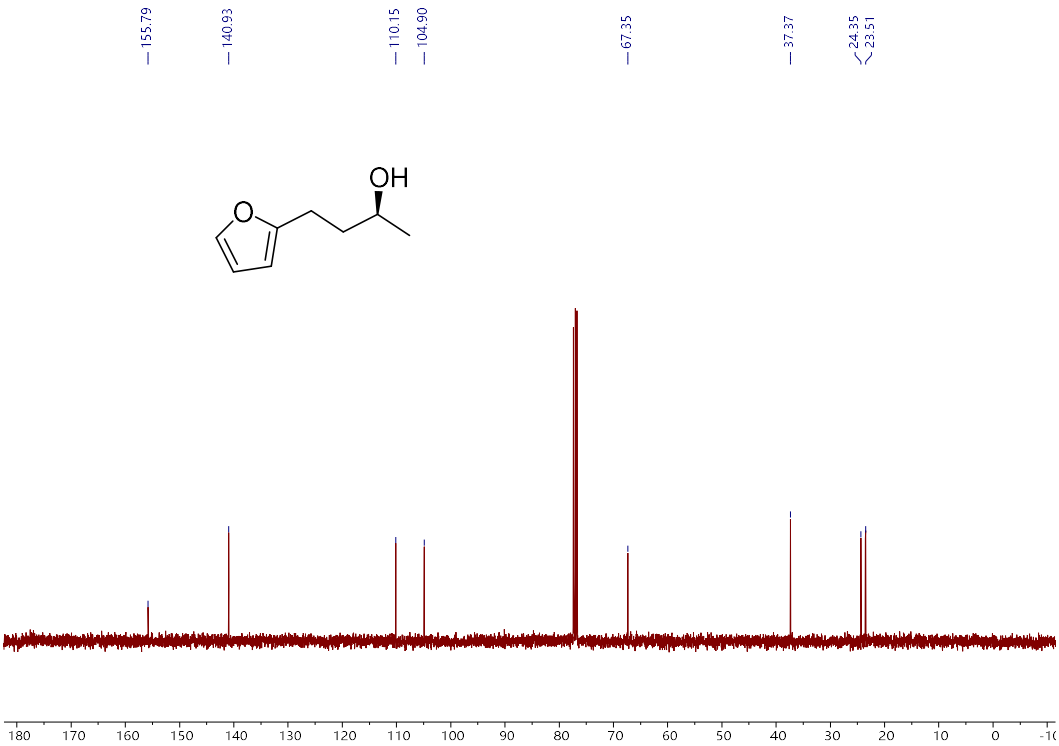
155.79
140.93
110.15
104.90
67.35
37.37
24.35
23.51
OH
O
180
170
160
150
140
130
120
110
100
90
80
70
60
50
40
30
20
10
0

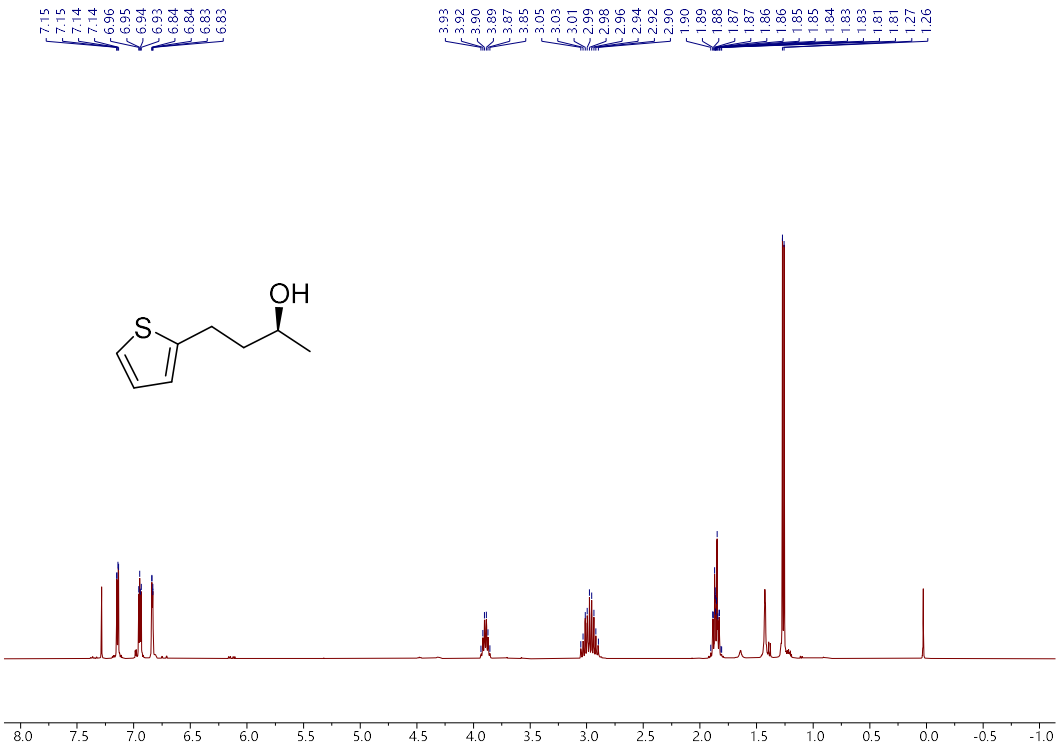
7.15
7.15
7.14
7.14
6.96
6.95
6.94
6.93
6.84
6.84
6.83
6.83
3.93
3.92
3.90
3.89
3.87
3.85
3.05
3.03
3.01
2.99
2.98
2.96
2.94
2.92
2.90
1.90
1.89
1.88
1.87
1.87
1.86
1.86
1.85
1.85
1.84
1.83
1.83
1.81
1.81
1.27
1.26
OH
S
8.0
7.5
7.0
6.5
6.0
5.5
5.0
4.5
4.0
3.5
3.0
2.5
2.0
1.5
1.0
0.5
0.0
-0.5
-1.0

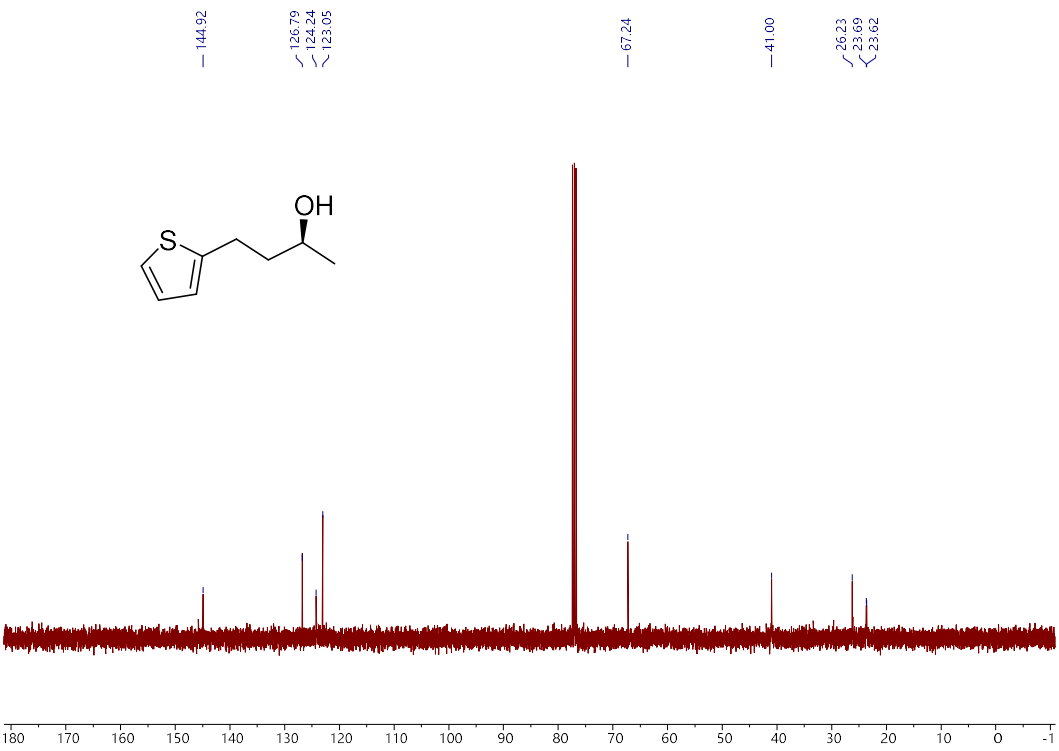
144.92
126.79
124.24
123.05
67.24
41.00
26.23
23.69
23.62
OH
S
180
170
160
150
140
130
120
110
100
90
80
70
60
50
40
30
20
10
0
-1

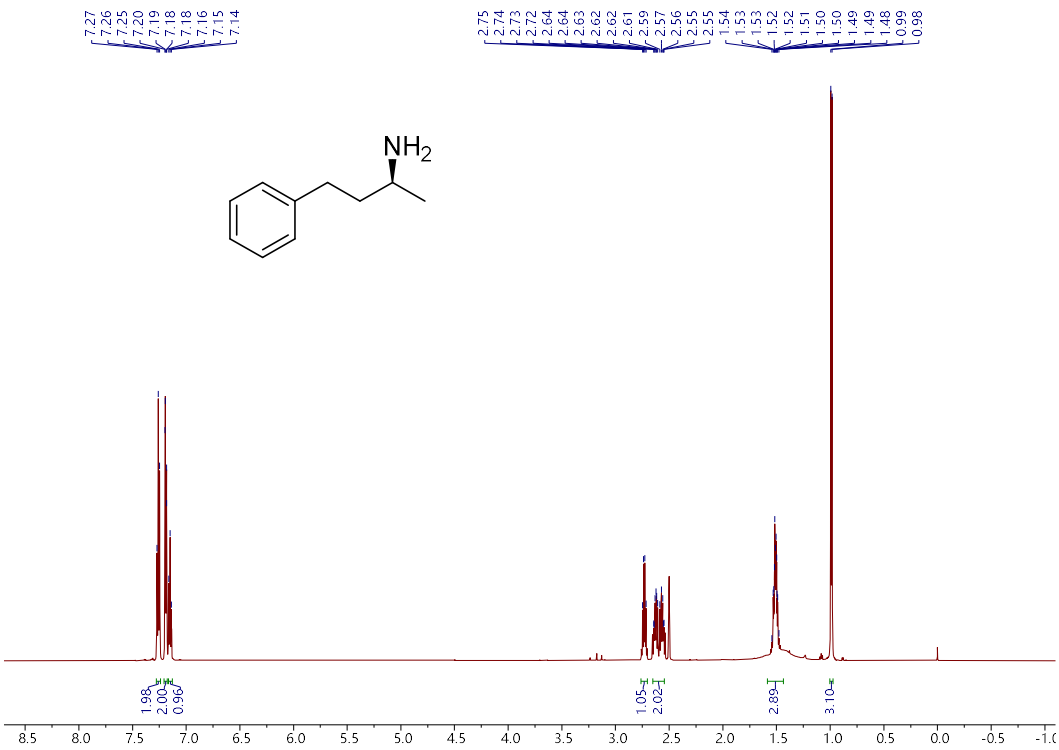
7.27
7.26
7.25
7.20
7.19
7.18
7.18
7.16
7.15
7.14
2.75
2.74
2.73
2.72
2.64
2.64
2.63
2.62
2.62
2.61
2.59
2.57
2.56
2.55
2.55
1.54
1.53
1.53
1.52
1.52
1.51
1.50
1.50
1.49
1.49
1.48
0.99
0.98
NH2
1.98
2.00
0.96
1.05
2.02
2.89
3.10
8.5
8.0
7.5
7.0
6.5
6.0
5.5
5.0
4.5
4.0
3.5
3.0
2.5
2.0
1.5
1.0
0.5
0.0
-0.5

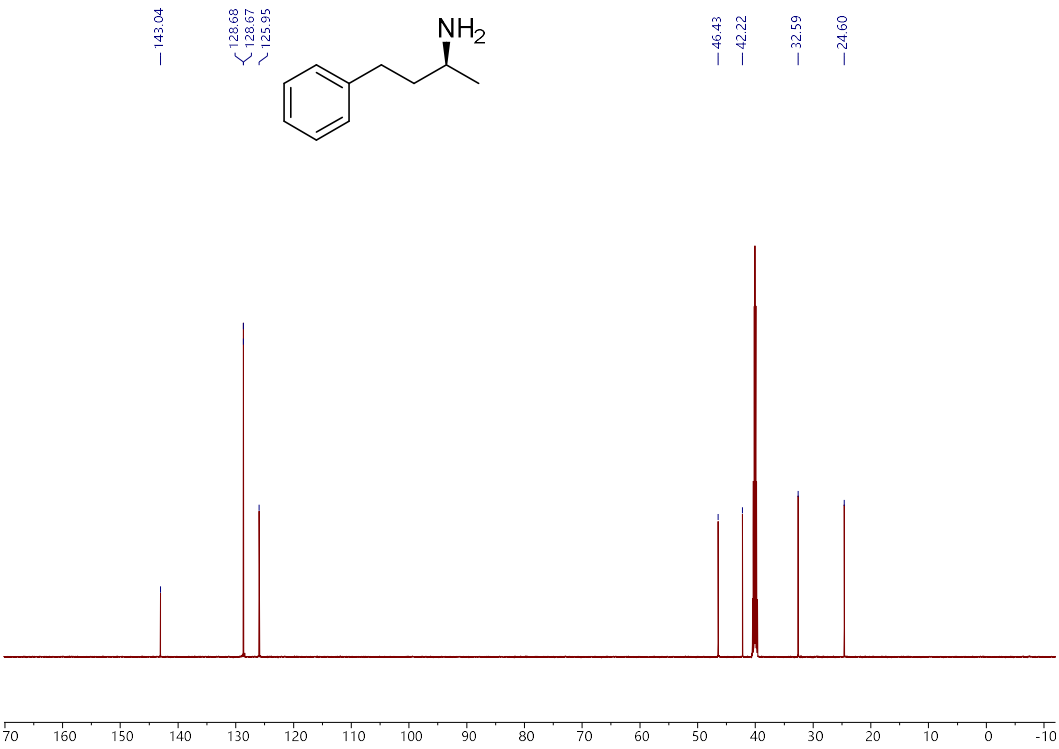
143.04
128.68
128.67
125.95
NH2
46.43
42.22
32.59
24.60
70
160
150
140
130
120
110
100
90
80
70
60
50
40
30
20
10
0
-10

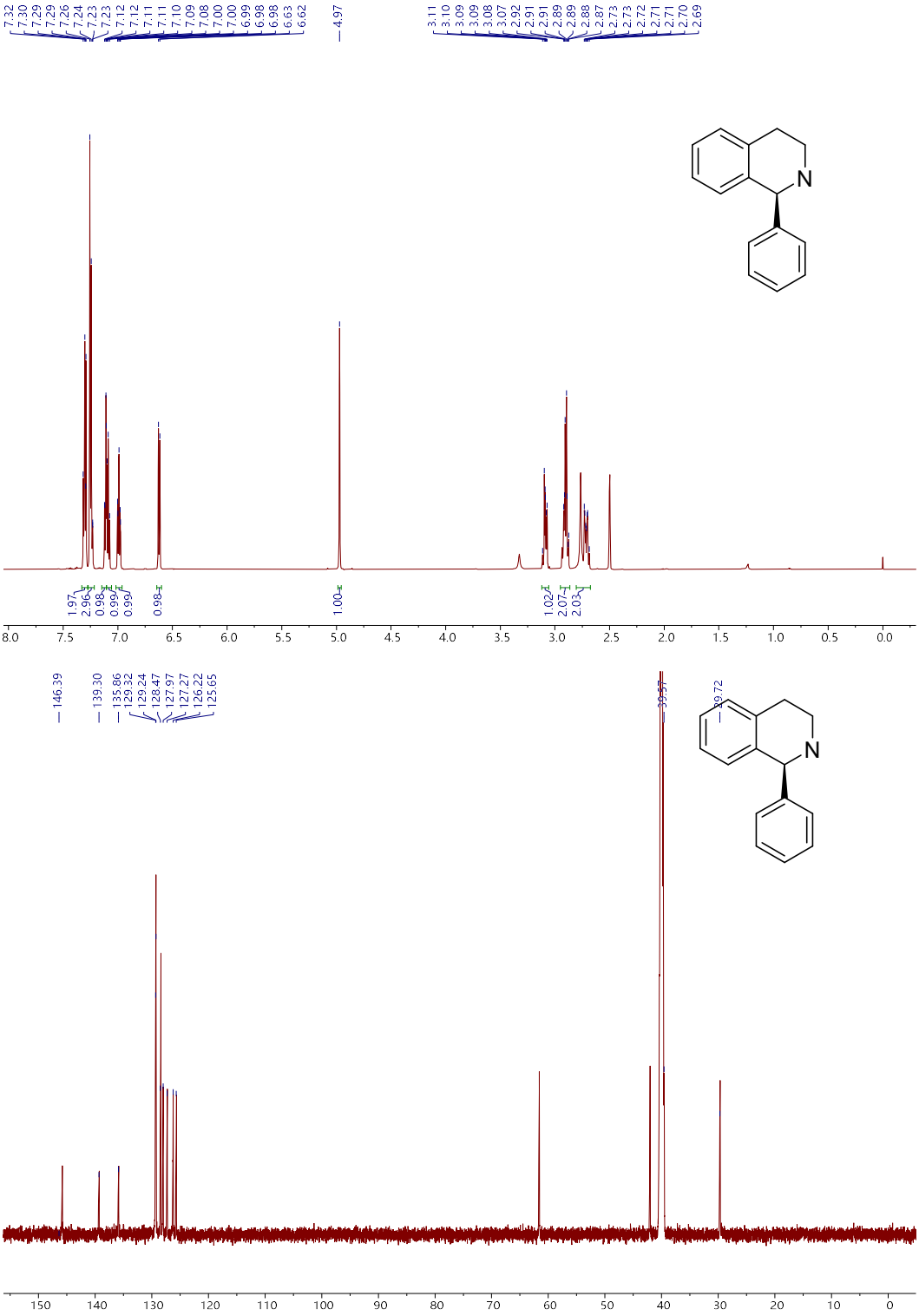
7.32
7.30
7.29
7.29
7.26
7.24
7.23
7.23
7.12
7.12
7.11
7.11
7.10
7.09
7.08
7.00
7.00
6.99
6.98
6.98
6.63
6.62
4.97
3.11
3.10
3.09
3.09
3.08
3.07
2.92
2.91
2.91
2.89
2.89
2.88
2.87
2.73
2.73
2.72
2.71
2.71
2.70
2.69
N
1.97
2.96
0.98
0.99
0.99
0.98
1.00
1.02
2.07
2.03
8.0
7.5
7.0
6.5
6.0
5.5
5.0
4.5
4.0
3.5
3.0
2.5
2.0
1.5
1.0
0.5
0.0
146.39
139.30
135.86
129.32
129.24
128.47
127.97
127.27
126.22
125.65
39.97
29.72
N
150
140
130
120
110
100
90
80
70
60
50
40
30
20
10
0

GC traces for products

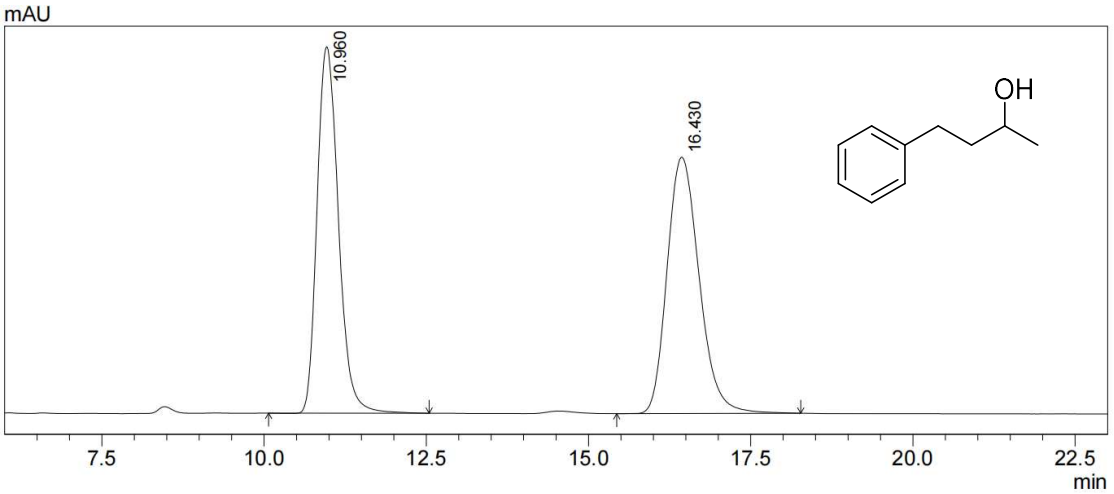

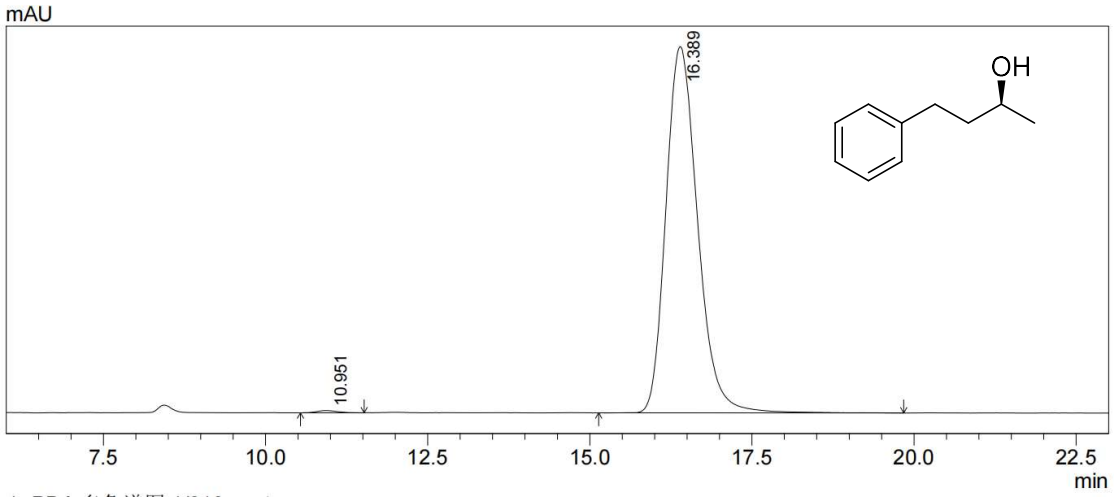

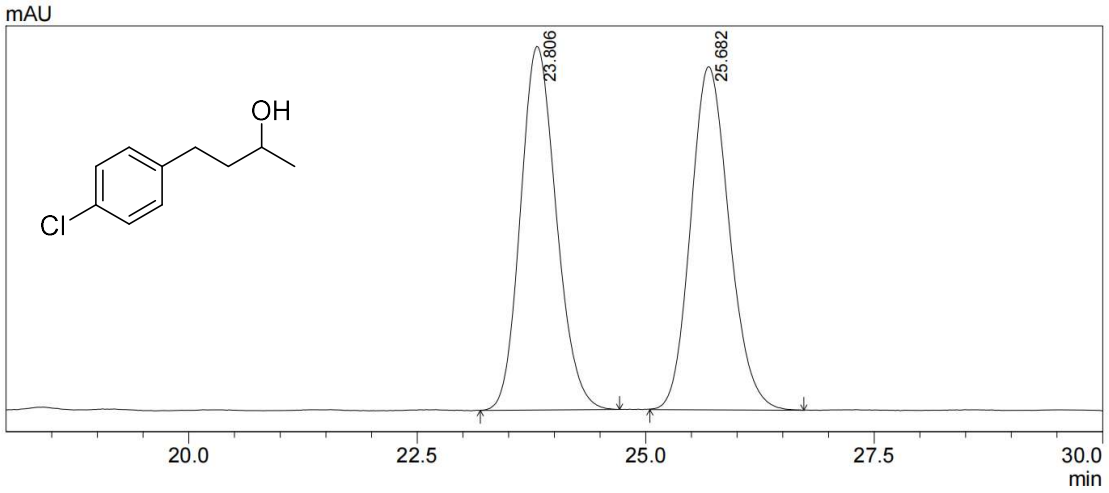
mAU
23.806
25.682
OH
Cl
20.0
22.5
25.0
27.5
30.0
min

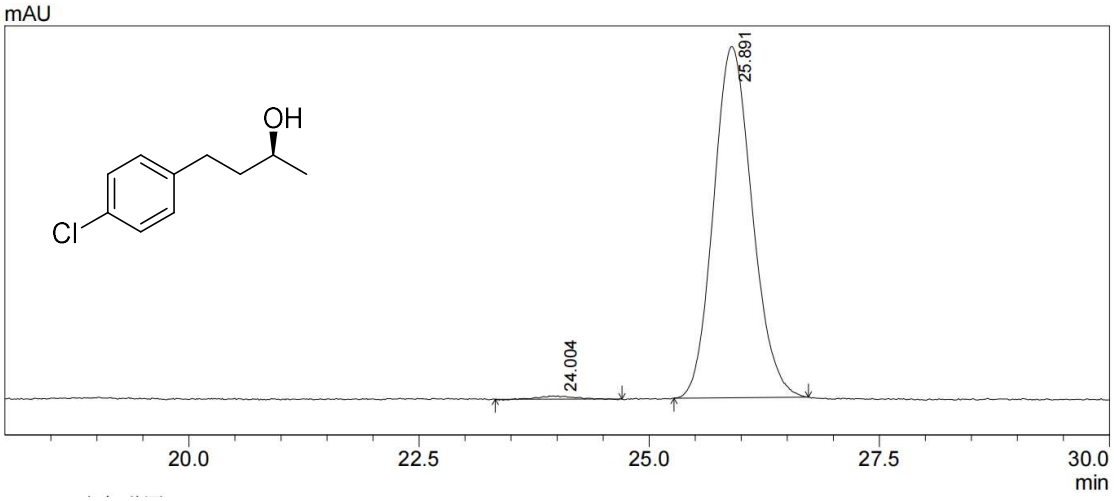
mAU
25.891
24.004
OH
Cl
20.0
22.5
25.0
27.5
30.0
min

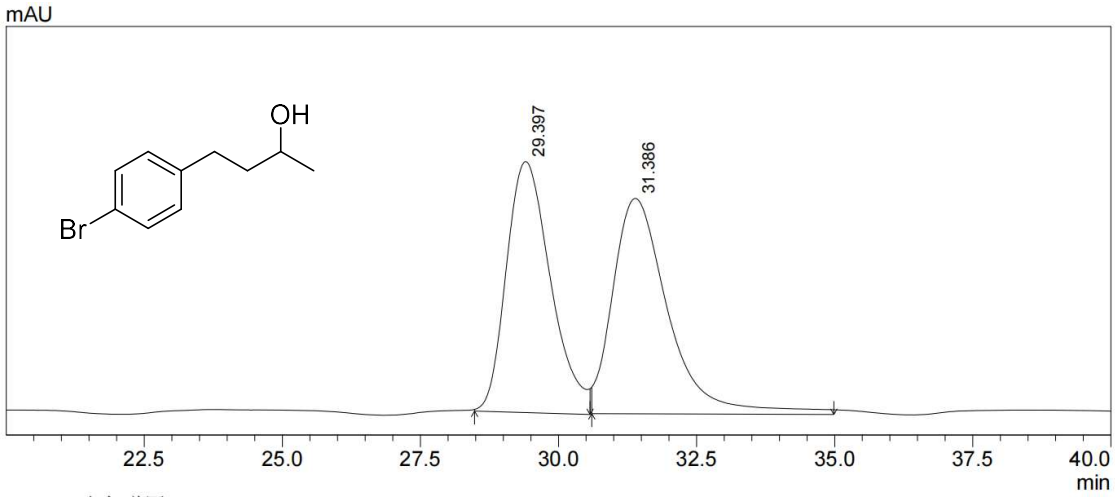
mAU
OH
Br
29.397
31.386
22.5
25.0
27.5
30.0
32.5
35.0
37.5
40.0
min

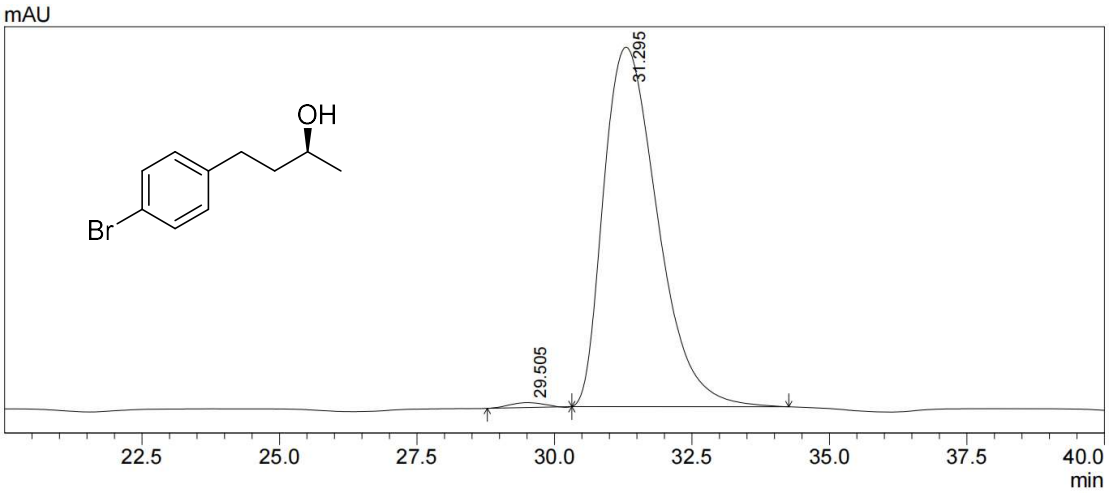
mAU
OH
Br
31.295
29.505
22.5
25.0
27.5
30.0
32.5
35.0
37.5
40.0
min

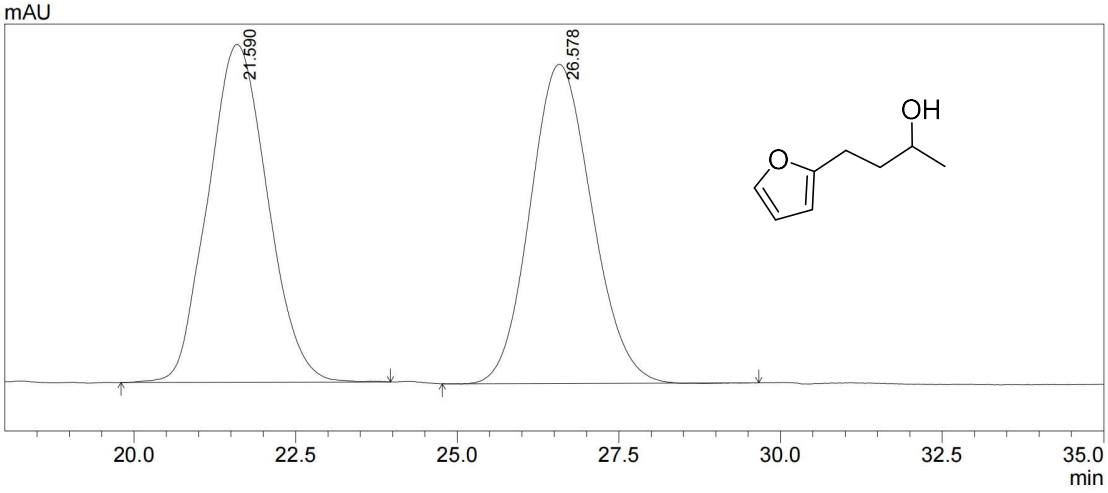
mAU
21.590
26.578
OH
O
20.0
22.5
25.0
27.5
30.0
32.5
35.0
min

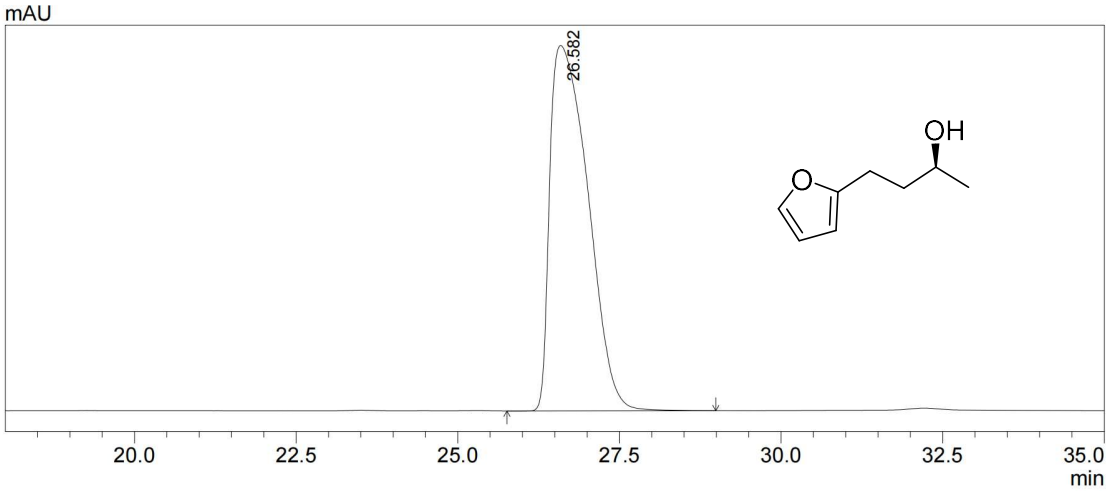
mAU
26.582
OH
O
20.0
22.5
25.0
27.5
30.0
32.5
35.0
min

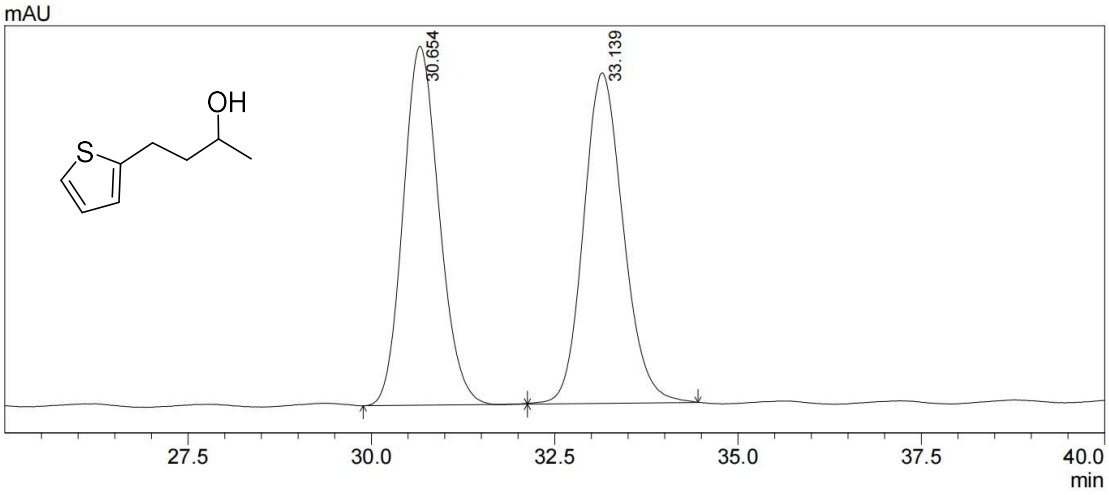
mAU
30.654
33.139
OH
S
27.5
30.0
32.5
35.0
37.5
40.0
min

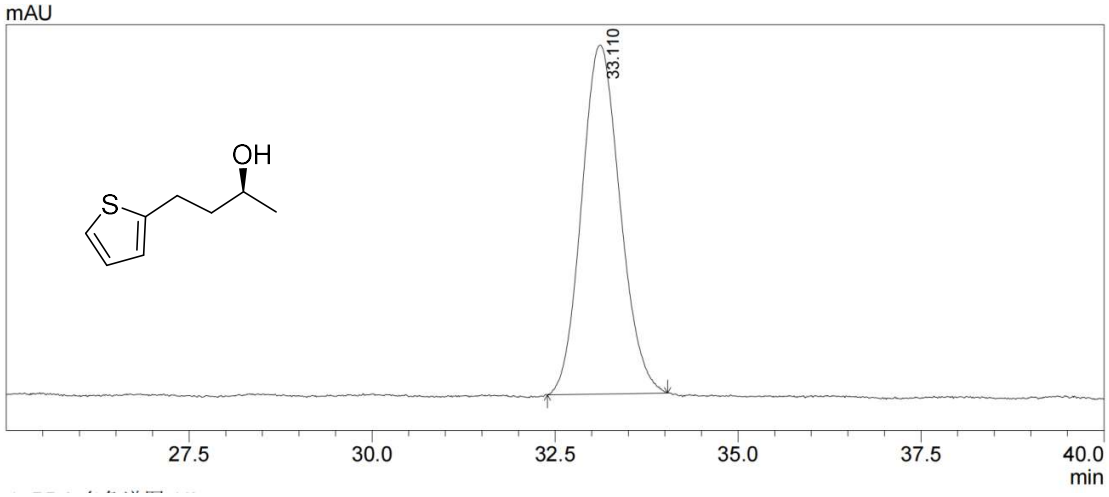
mAU
33.110
OH
S
27.5
30.0
32.5
35.0
37.5
40.0
min

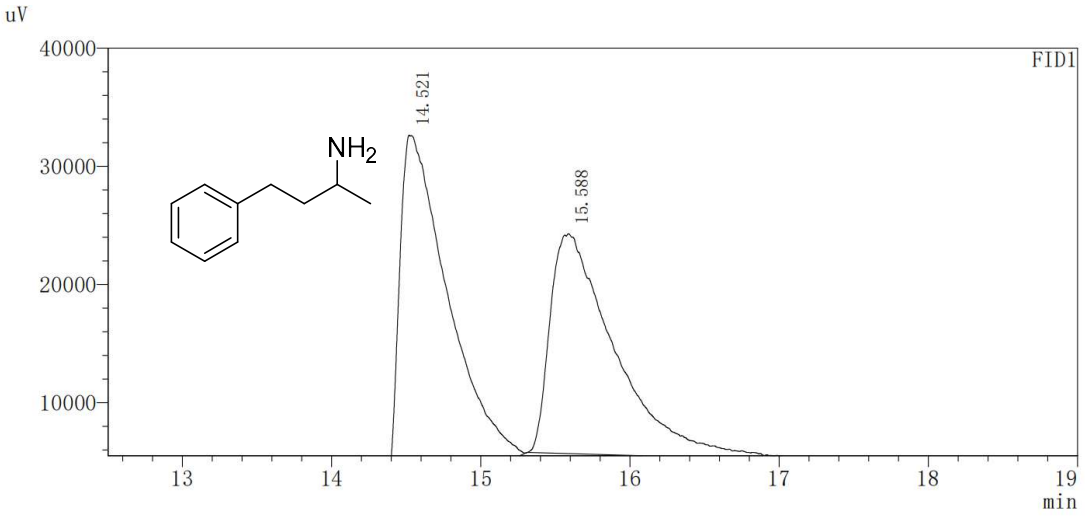
uV
40000
30000
20000
10000
FID1
14.521
15.588
NH2
13
14
15
16
17
18
19
min

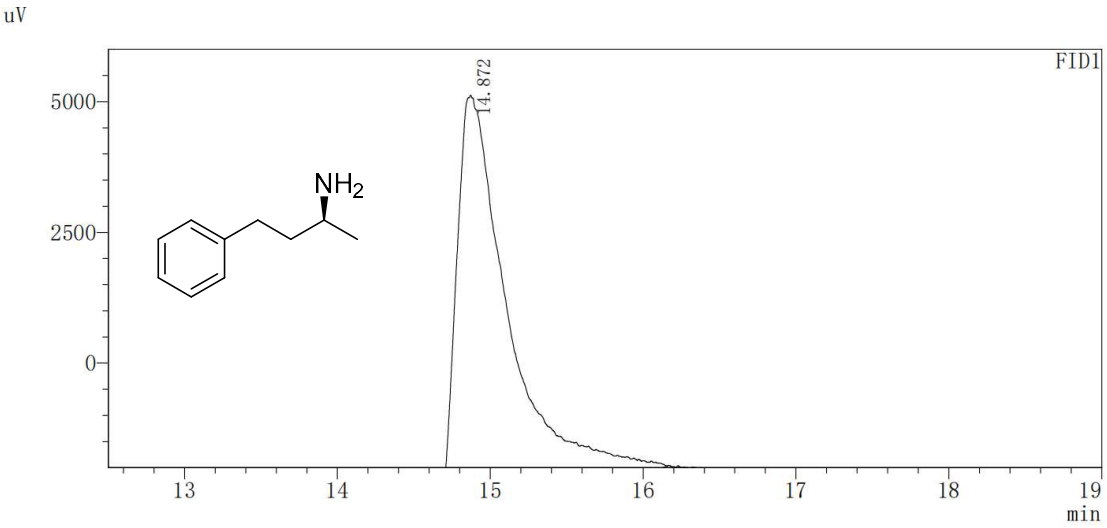
uV
5000
2500
0
FID1
14.872
NH2
13
14
15
16
17
18
19
min

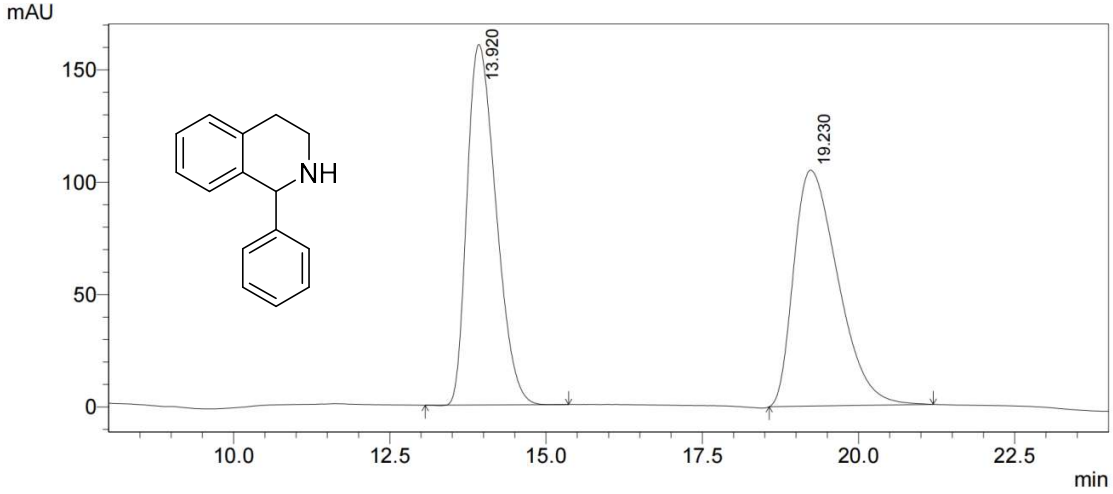
mAU
150
100
50
0
13.920
19.230
NH
10.0
12.5
15.0
17.5
20.0
22.5
min

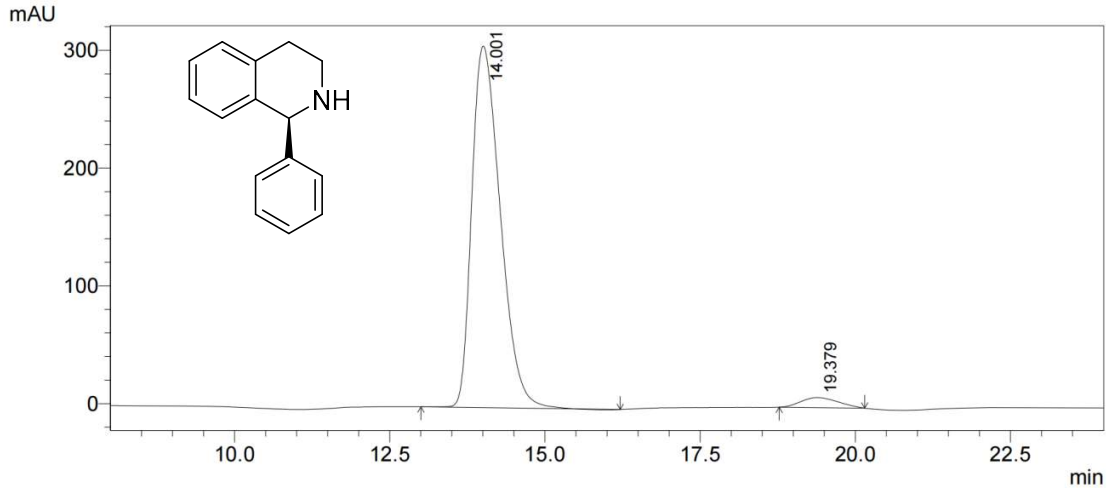
mAU
300
200
100
0
14.001
19.379
NH
10.0
12.5
15.0
17.5
20.0
22.5
min

Reference:

1. Liu, Z.; Huang, F.; Peng, M.; Chen, Y.; Cai, X.; Wang, L.; Hu, Z.; Wen, X.; Wang, N.; Xiao, D.; Jiang, H.; Sun, H.; Liu, H.; Ma, D., Tuning The Selectivity of Catalytic Nitriles Hydrogenation by Structure Regulation in Atomically Dispersed Pd Catalysts. *Nat. Commun.* **2021,** *12* (1), 6194.

2. Liang, Q.; Li, W.; Xie, L.; He, Y.; Qiu, B.; Zeng, H.; Zhou, S.; Zeng, J.; Liu, T.; Yan, M.; Liang, K.; Osamu, T; Jiang, L.; Kong, B., General Synergistic Capture-Bonding Superassembly of Atomically Dispersed Catalysts on Micropore-Vacancy Frameworks. *Nano Lett.* **2022,** *22* (7), 2889-2897.

3. Xie, J.; Cheng, J.; Peng, J.; Zhang, J.; Wu X.; Zhang, R.; Li, Z.; Li, C., A Tandem Catalysis for Isoindolinone Synthesis over Single-Atom Pd TiO_2 Catalyst. *Angew. Chem. Int. Ed.* **2024,** e202415203.

4. Chen, L.; Allec, S. I.; Nguyen, M-T.; Kovarik, L.; Hoffman, A. S.; Hong, J.; Meira, D.; Shi, H.; Bare, S. R.; Glezakou, V-A.; Rousseau, R.; Szanyi, J., Dynamic Evolution of Palladium Single-Atoms on Anatase Titania Support Determines the Reverse Water Gas. *J.Am.Chem.Soc.* **2023,** *145* (19), 10847−10860.

5. Liu, P.; Zhao, Y.; Qin, R.; Mo, S.; Chen, G.; Gu, L.; Chevrier, D. M.; Zhang, P.; Qing Guo; Zang, D.; Wu, B.; Fu, G.; Zheng, N., Photochemical Route for Synthesizing Atomically Dispersed Palladium Catalysts. *Science* **2016,** *352* (6287).

6. He, Q.; Lee, J.; Liu, D.; Liu, Y.; Lin, Z.; Xie, Z.; Hwang, S.; Kattel, S.; Song, L.; Chen, J. G., Accelerating CO_2 Electroreduction to CO Over Pd Single-Atom Catalyst. *Adv. Funct. Mater.* **2020,** *30* (17), 2000407.

7. Yang, W.; Felipe, P; Zhou, H.; Huang, Z.; Ch,i M.; Meyer, I.H.; Yu, X.; Li, Y.; Wu, Z., Boosting the Activity of Pd Single Atoms by Tuning Their Local Environment on Ceria for Methane Combustion. *Angew. Chem. Int. Ed.* **2022,** *62* (5), e202217323.

8. Zhou, S.; Shang, L.; Zhao, Y.; Shi, R.; Waterhouse, G. I. N.; Huang, Y.; Zheng, L.; Zhang, T., Pd Single-Atom Catalysts on Nitrogen-Doped Graphene for the Highly Selective Photothermal Hydrogenation of Acetylene to Ethylene. *Adv. Mater.* **2019,** *31* (18), 1900509.

9. Ren, X.; Li, C.; Liu, J.; Li, H.; Bing, L.; Bai, S.; Xue, G.; Shen, Y.; Yang, Q., The Fabrication of Pd Single Atoms/Clusters on COF Layers as Cocatalysts for Photocatalytic H_2 Evolution. *ACS Appl. Mater. Interfaces.* **2022,** *14* (5), 6885−6893.

10. Zhao, Q.; Zhao, X.; Liu, Z.; Ge, Y.; Ruan, J.; Cai, H.; Zhang, S.; Ye, C.; Xiong, Y.; Chen, W.; Meng, G.; Liu, Z.; Zhang, J., Constructing Pd and Cu Crowding Single Atoms by Protein Confinement to Promote Sonogashira Reaction. *Adv. Mater.* **2024,** *36* (36), 2402971.

11. Tao, X.; Long, R.; Wu, D.; Hu, Y.; Qiu, G.; Qi, Z.; Li, B.; Jiang, R.; Xiong, Y., Anchoring Positively Charged Pd Single Atoms in Ordered Porous Ceria to Boost Catalytic Activity and Stability in Suzuki Coupling Reactions. *Small* **2020,** *16* (43), 202001782.

12. Ma, Y.; Ren, Y.; Zhou, Y.; Liu, W.; Baaziz, W.; Ersen, O.; Pham-Huu, C.; Greiner, M.; Chu, W.; Wang, A.; Liu, T., High-Density and Thermally Stable Palladium Single-Atom Catalysts for Chemoselective Hydrogenations. *Angew. Chem. Int. Ed.* **2020,** *59* (48), 21613–21619.

13. Li, X.; Cao, Y.; Luo, K.; Zhang, L.; Bai, Y.; Xiong, J.; Zare, R. N.; Ge, J., Cooperative Catalysis by a Single-Atom Enzyme-Metal Complex. *Nat. Commun.* **2022,** *13* (1), 2189.

14. Pedireddy, S.; Jimenez-Sandoval, R.; Ravva, M. K.; Nayak, C.; Anjum, D. H.; Jha, S. N.; Katuri, K. P.; Saikaly, P. E., Harnessing the Extracellular Electron Transfer Capability of Geobacter sulfurreducens for

Ambient Synthesis of Stable Bifunctional Single-Atom Electrocatalyst for Water Splitting. *Adv. Funct. Mater.* **2021,** *31* (22), 2010916.